# Chapter one

# Introduction

## 1.1 historical backgrounds:

X-ray computed tomography, also computed tomography (CT scan), computed axial tomography (CAT scan) or computer assisted tomography is a medical imaging procedure that uses computer-processed X-rays to produce tomographic_images or 'slices' of specific areas of the body. These cross-sectional images are used for diagnostic and therapeutic purposes in various medical disciplines (Merriam-Webster on line dictionary). Digital geometry_processing is used to generate a three-dimensional image of the inside of an object from a large series of two-dimensional X-ray images taken around a single axis of rotation (Hermam,G. T 2009).

One of the most important functions of a computed tomography (CT) system is to reproduce a three dimensional structure and represent that structure as an accurate two-dimensional cross-section on a television monitor. There are several characteristics that effect how well a CT system performs this task. Spatial resolution, contrast resolution, linearity, noise and artifacts are the primary characteristics that effect image quality in CT (Will reddinger 1998).

Enhancing or suppressing any of these characteristics depends upon the imaging interests and the region of the body being scanned.

The radiation dose reported in the gray or mGy unit is proportional to the amount of energy that the irradiated body part is expected to absorb, and the

physical effect (such as DNA double strand breaks) on the cells' chemical bonds by x-ray radiation is proportional to that energy(Polo SE, Jackson SP (March 2011).

The sievert unit is used in the report of the effective_dose. The sievert unit in the context of CT scans, does not correspond to the actual

radiation dose that the scanned body part absorbs, but rather to another radiation dose of another scenario, in which the whole body absorbs the other radiation dose, and where the other radiation dose is of a magnitude that is estimated to have the same probability to induce cancer as the CT scan (Report of AAPM task group 23(January 2008)). Thus, the actual radiation that is absorbed by a scanned body part is often much larger than the effective dose suggests. A specific measure, termed the computed tomography dose index (CTDI), is commonly used as an estimate of the radiation absorbed dose for tissue within the scan region, and is automatically computed by medical CT scanners.

The equivalent dose is the effective dose of a case, in which the whole body would actually absorb the same radiation dose, and the sievert unit is used in its report. In the case of non-uniform radiation, or radiation given to only part of the body, which is common for CT examinations, using the local equivalent dose alone would overstate the biological risks to the entire organism.

## 1.2 **Objectives of the study:**

To adapt proper brain protocol to produce good image quality with minimum radiation dose.

To correlate between image quality and radiation dose.

To correlate between CT brain protocols and radiation dose.

## 1.3 Problem of the study:

CT provides high image quality, but associated with high radiation dose this radiation dose can be reduced by manipulated scan protocol parameters.

# Chapter two

# Theoretical background

## 2.1 CT back ground:

### 2.1.1 CT scanning the early days

It is less than 34 years ago, on 20th April 1972 that an unknown engineer from EMI Ltd, the company better known at the time for publishing the Beatles records, gave a presentation at the 32nd Congress of the British Institute of Radiology. The Engineer, Godfrey Hounsfield, was lecturing with Dr James Ambrose from Atkinson Morley's Hospital on “Computerized Axial Tomography (A new means of demonstrating some of the soft tissue structures of the brain without the use of contrast media)” [ (*Hounsfield GN1973)*,( *Ambrose J.1973*)]. Many people attending that BIR congress will never forget the experience of hearing a presentation on CT scanning for the first time. In fact Hounsfield had presented the results of some of his animal experiments the previous year at the 2nd congress of the European Association of Radiology, in Amsterdam, but they had not excited much interest. The same might have happened in the USA because at a Neuro Postgraduate Course at the Albert Einstein College of Medicine, New York, on Monday 15th May 1972, only about a dozen people stayed to hear an extra lunchtime lecture by Hounsfield and Dr Bull, where they showed the first clinical images. However these people realized the significance of what they had seen and the news spread rapidly.

### 2.1.2 The beginning:

In the mid 1960s Hounsfield was working on the pattern recognition of letters when he began to consider whether he could reconstruct a three-dimensional representation of the contents of a box from a set of readings taken through the box at randomly selected directions. He found that by considering the three-dimensional object within the box as a series of slices, reconstruction was easier than treating the content as a volume.

He tested the theoretical principal by working with a matrix of numbers set to zero with a square in the middle where each number was set at 1000. He entered these data into a computer program to get simulated absorption values and then reconstructed the picture using another program. Hounsfield recalled his surprise at how accurate the result was.

### 2.1.3 The project proposal:

Once Hounsfield had proved the theoretical principle he went on to generate the original project proposal in 1968. Here he stated “The purpose of the study was to investigate the employment of a computer to make better use of the information obtained when an object is examined by gamma rays or X-rays”. In this proposal Hounsfield compared the classic conventional X-ray technique producing a confused and fuzzy picture to the clear outline produced by the proposed system. Hounsfield proposed a system as shown in Figure 2.1.1 based upon reconstructing pictures of slices through an object and in detailing the expected benefits he indicated a theoretical accuracy of detection better than 1%.

**Figure 2.1.1**

**Extract of the original 1968 project proposal(BJR)**

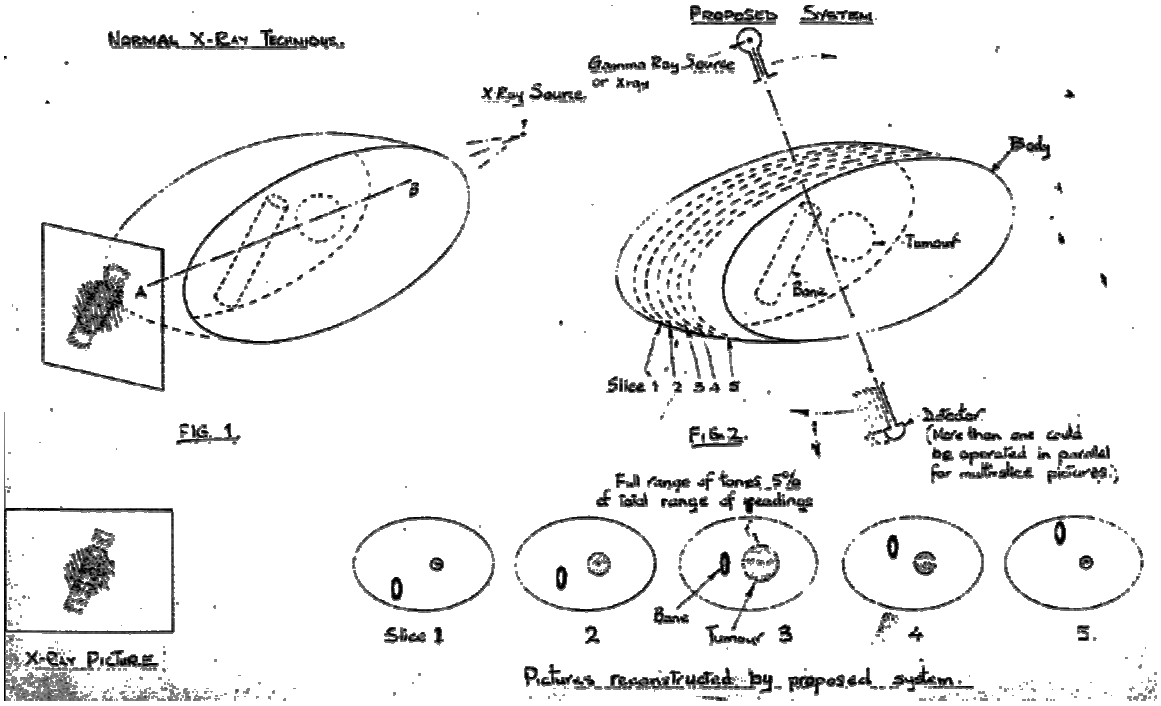


## 2.1.4 The lathe bed model:

The initial test rig was built on the bed of an old lathe which Hounsfield had been using in a previous project working on computer stores. Hence the early test unit became referred to as the “Lathe bed model”. The initial rig utilized a gamma source, Americium 95, with a photon counter as the detector. On this rig, the source made 160 traverses of the object, which was rotated 1° at the end of each traverse for a total of 180°. It took 9 days to collect sufficient information, and 2.5 h to reconstruct the image on an ICL 1905 mainframe computer. However, the resultant images proved the feasibility of the technique and with the replacement of the gamma source

by an X-ray source as shown in Figure 2.1.2, the scanning time was reduced to 9 h.

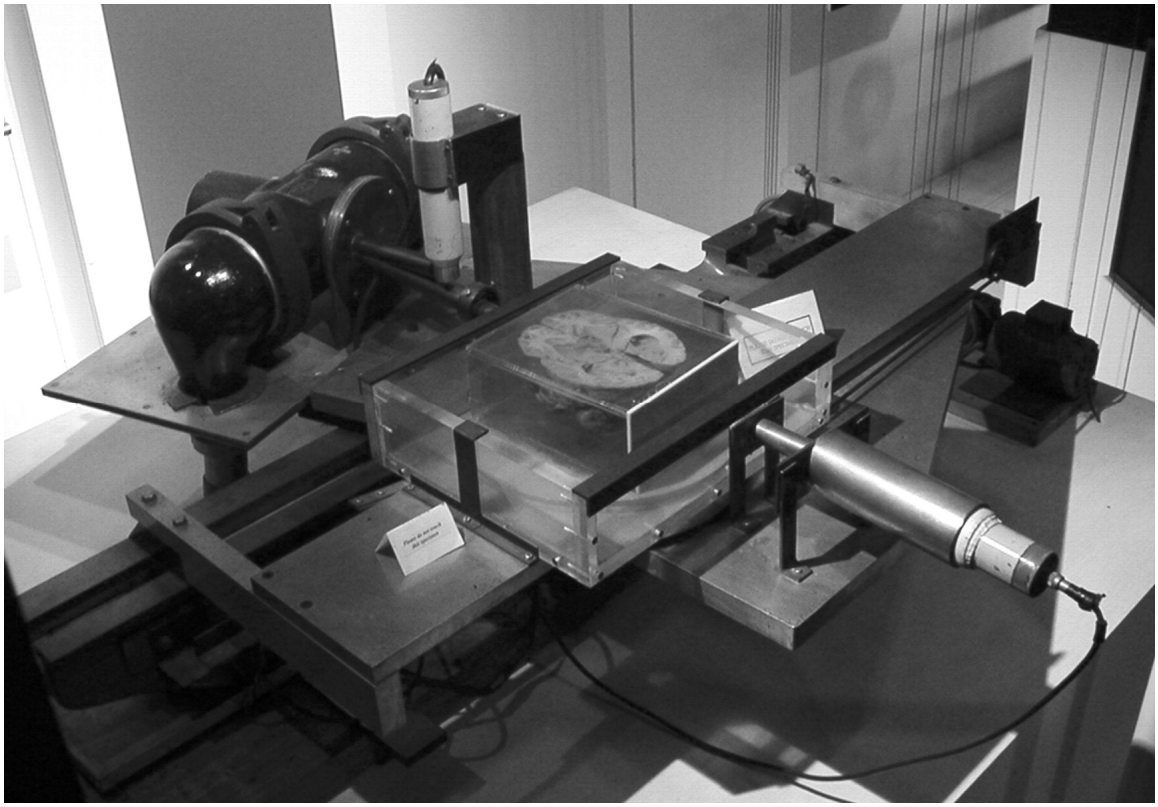

**Figure 2.1.2**

The original lathe bed model (copyright EMI Ltd).(BJR)

Initial images were of inert objects, then specimens from an abattoir, including bullocks brains and pigs bodies as shown in Figure 2.1.3. Due to the long scan times, particularly with the gamma source, many of these specimens decayed while the pictures were acquired producing gas bubbles which caused artifacts in the images. This initial work was done by a very small team comprising Hounsfield, Stephen Bates (programming), Peter Langstone (electronics) and Mel King (mechanics) working on a very low budget of £25 000.

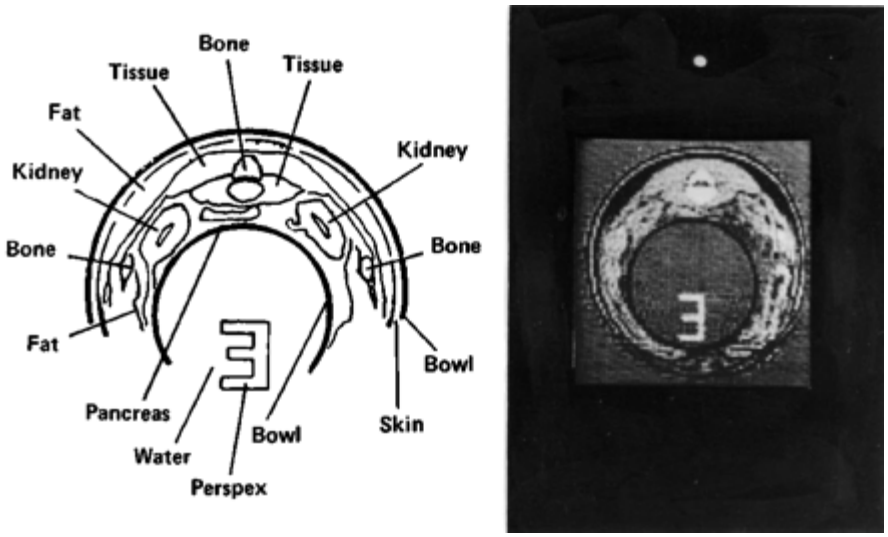


**Figure 2.1.3**

Early scan of a pig.(BJR)

Dr James Ambrose recalls that, in about 1969, he received a call from an old acquaintance, Dr Evan Lennon then principal medical officer in Radiology at the Department of Health, asking if he would see a man called "Godfrey Hounsfield" and listen to him. Lennon had found him confusing but was reluctant to dismiss him as a crank (Ambrose later learnt that other eminent radiologists had already dismissed him as a crank!). Ambrose recalls that when he and his senior physicist Dr John Perry met Hounsfield, the conversation was difficult. Hounsfield would only say that the method was fundamentally different from other methods of X-ray imaging, more efficient in photon usage and likely to be more sensitive to small density variations. In order to demonstrate a clinically relevant image, Ambrose arranged for a bottled specimen of a brain to be borrowed from a museum

and was amazed at the image Hounsfield showed him 5 weeks later. An image of the first brain scanned is shown in Figure 2.1.4

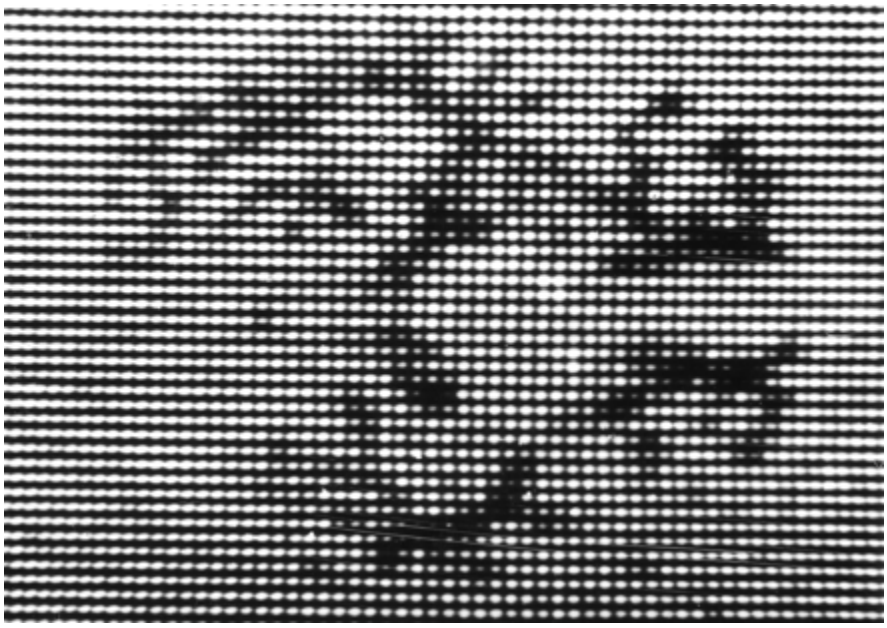

**Figure 2.1.4**

First image of a brain specimen.(BJR)

### 2.1.5Building the prototype

Having shown some clinically interesting images the project was then ready to move to the next stage of building a full prototype. However funding was an issue. It was Gordon Higson at the Department of Health who had the foresight to place an order for a machine with a theoretical specification which included a 4–5 min scan time and an 0.5% pixel accuracy, and this enabled the project to continue. This order was for a prototype and three clinical machines that would generate sufficient income to fund a fifth machine for Hounsfield and his team to keep and work on. The Department of Health order would also fund half the remaining research costs and in

exchange they would receive a small royalty on sales. At the time it was calculated that it would cost £69 000 to build a complete working system and so it was agreed that the Department of Health would pay £150 000 for each of the four systems.

### 2.1.6 The first clinical patient:

The prototype was installed at Atkinson Morley's Hospital in South London where the first patient, a middle aged lady with a suspected frontal lobe tumor, was scanned on 1st October 1971. The surgeon who operated on her shortly afterwards reported that “it looks exactly like the picture” shown in Figure 2.1.5

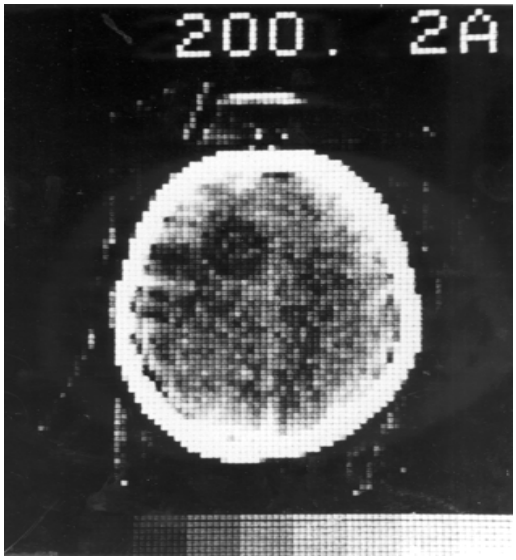


**Figure 2.1.5**

First patient image scanned on the prototype EMI scanner at Atkinson Morley's Hospital on 1st October 1971.(BJR)

Hounsfield remained cautious. He recalled “I've had this before, first time is always lucky and then everything else goes wrong after that. So I thought,

the next ones are not going to be any good, but they did another ten more patients and every one of them came out as being obvious diseases of the brain showing up in various forms. Dr Ambrose found that, by injecting iodine-based contrast agent that would localize the particular spot where the tumor was and it showed up even better". Hounsfield took some of the contrast enhanced images and subtracted without contrast images to compare the blood flow on either side of the brain.

In the original system the patient's head was placed in a rubber cap surrounded by water. This water bag was used to reduce the dynamic range of the detected X-rays and improve the absolute values of the attenuation figures.

Using one sodium iodide (NaI) crystal and photomultiplier tube detector per slice, plus one as a reference detector with a scan time of 4.5–20 min per 180° scan, the system acquired two contiguous slices per scan each with a 80 × 80 matrix of 3 mm × 3 mm × 13 mm voxels. Early images showed the ability to meet the pixel density accuracy of 0.5% in the absorption coefficient as defined in the theoretical specification.

The three systems ordered by the Department of Health were installed at the National Hospital for Neurology and Neurosurgery in London, Manchester and Glasgow. After this, the first CT scanners were installed in the USA at the Massachusetts General Hospital and the Mayo Clinic, where the first scan in the USA was done on 19th June 1973.

### 2.1.7 Reconstructing the picture:

Early scan data were actually taken back to EMI on tape for processing overnight which took 20 min per image on an ICL 1905 computer. In production this was done on a mini-computer which fortuitously had emerged at the right time. Images were taken back the next day on tape to Atkinson Morley's Hospital to be displayed. The early images were displayed in three ways; paper printout, cathode ray tube (CRT) display or as a Polaroid picture of the CRT display.

The early images were generated using iterative algebraic reconstruction implemented by Steve Bates on the ICL 1905 mainframe. Subsequently reconstruction used the filtered back projection or convolution method invented and patented by Chris Lemay, one of the many patents filed and held by Hounsfield and his team. On the original EMI Mk1 scanner an 80 × 80 image took 7 min to process, with filtered back projection on the same computer a 160 × 160 image could be processed in 30 s after the end of the scan.

It had been thought that image reconstruction and processing was so complicated that it would have to be done at a central processing unit on a suitable large and fast main frame machine.

But the introduction of the minicomputer and the implementation of the new improved reconstruction algorithms were to change this.

### 2.1.8 CT1010 scanner:

A challenge with the original EMI Mk1 scanner was the water bag, both as regards the ease of use with patients and also due to the occasional water

leak! Replacement of the water bag with shaped carbon fiber wedges and bean bags was a significant improvement. This was further enhanced by the increase to eight detectors per slice in the CT1010 which was still a two contiguous slice scanner offering 160 × 160 and 320 × 320 matrix sizes over a 210 mm scan diameter and with the minimum scan time improved to 1 min. The prototype of this system was installed in 1975 at Atkinson Morley's Hospital and showed significant improvement in clinical image quality.

### 2.1.9 Body scanning:

The feasibility of body scanning was proved when a slim member of the EMI team, Tony Williams, was scanned in a head scanner.

The first body images taken in the body prototype machine were of Hounsfield himself on 20th December 1974. The first body images were shown to a meeting at the first International Conference on CT Scanning in Bermuda on Friday 14th March 1975, one of these images is shown in Figure 2.1.6

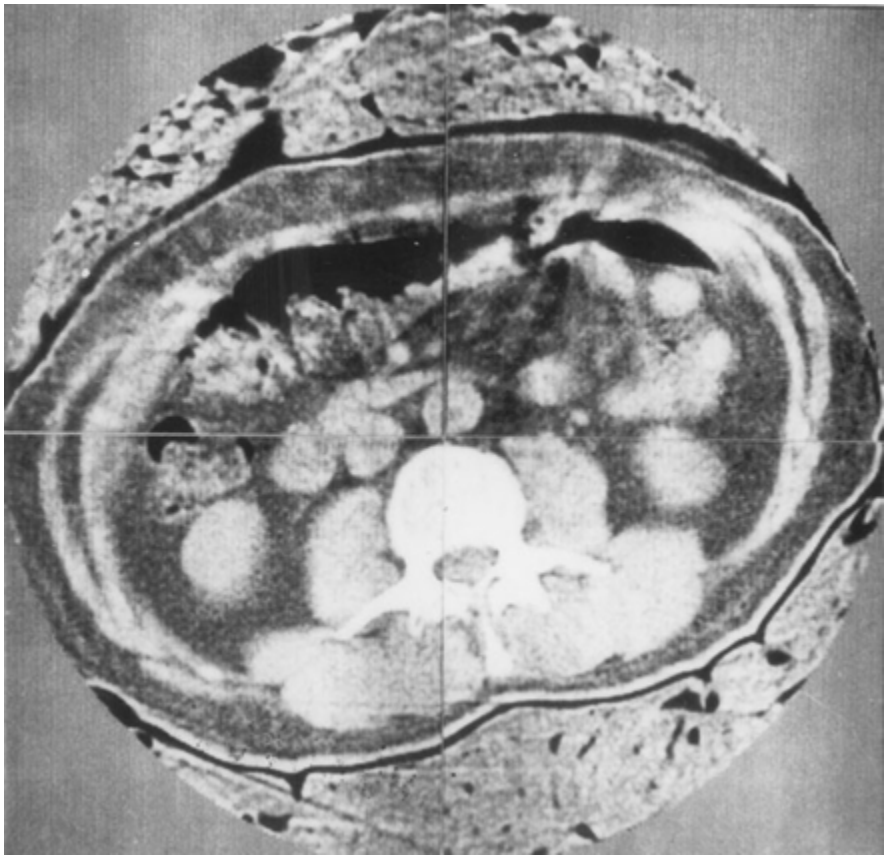

**Figure 2.1.6**

Body scan of Hounsfield taken on the prototype scanner in the laboratories and shown at Bermuda conference on 14th March 1975.(BJR)

All the research machines were named after stones: Opal, Pearl, Garnet and the body prototype was Emerald. This Emerald system was first installed clinically at Northwick Park Hospital in March 1975. The first body scan carried out in the USA was in October 1975 at the Mallinkrodt Institute St Louis. Dr Ron Evans recalled that this was a jaundiced patient, in whom it had been difficult to differentiate between medical and surgical jaundice. The CT scans showed that it was surgical jaundice which was subsequently clinically confirmed.

Initially known as the CT5000, the body scanner was developed into the commercial production machine, the CT5005. These body scanners were single slice machines using a gantry with 30 detectors plus a reference detector to reduce scan time to 20 s. The matrix had been increased to 320 × 320 over a selectable 240 mm, 320 mm or 400 mm scan field.

### 2.1.10 The generation game:

All these early scanners were the so called 1st or 2nd generation utilizing the translate/rotate technology where the gantry scanned across the patient before indexing by one degree and scanning back.

An early problem in CT scanner design was detector stabilization and the need for calibration. The EMI scanners were using NaI crystal photon detectors and photo multiplier tubes, and the translate/rotate technology enabled detector calibration by taking air readings at the end of each translate movement. This gave high accuracy but limited the speed of the scan. By 1976 there were 17 companies offering CT scanners with 3rd generation rotate/rotate scanners having been introduced, to offer fast scan times, most based upon xenon gas detectors arranged in an arc (*Brooks RA, Di Chiro G.1976*)[3].

Hounsfield realized the need for a system that was faster than translate/rotate and that could overcome the calibration and artifact issues of rotate/rotate systems.

### 2.1.11 Topaz:

The patent for a scanning focus system to produce a true volume scanner was filed on 19th October 1976. The Topaz research system, also named

after a stone and shown in Figure 2.1.7, was a 3rd generation system with a flying X-ray spot. The X-ray flying spot scanned in a direction opposite to the direction of rotation of the machine which meant that the body could be scanned with arcs of detector readings which overlapped in such a way that they could be compared and continuously calibrated. Built with 612 detectors including a central zoom region, Topaz had a resolution in the *x*-*y* plane of 0.65 mm. Volume scans taken in June 1980 were displayed in three dimensions in real time as 1200 × 1200 × 270 pixels.

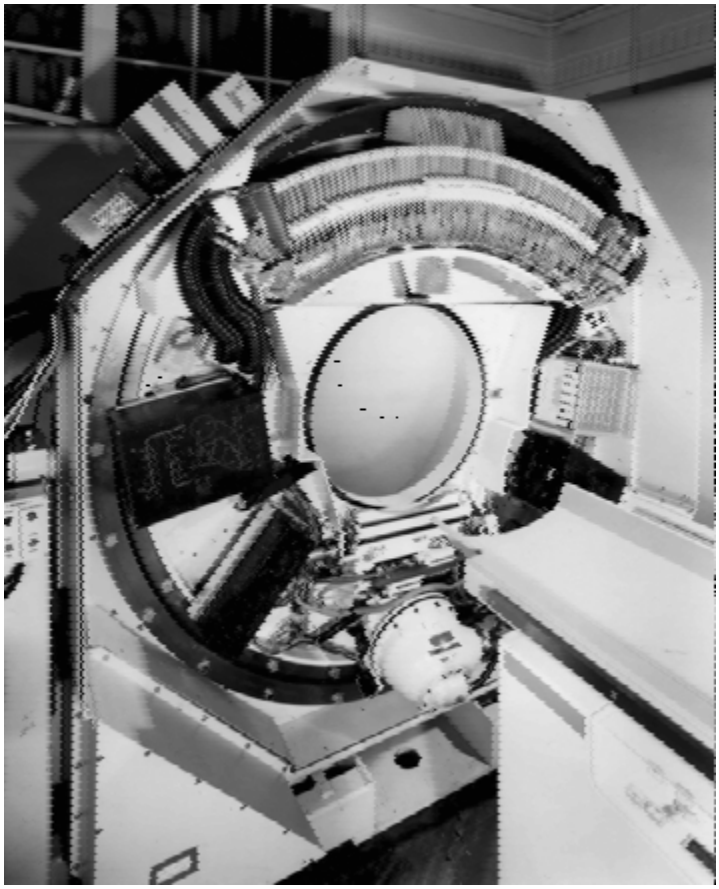

**Figure 2.1.7**

Topaz 3rd generation flying focal spot scanner.(BJR)

### 2.1.12 Recognition:

Initially the scale for describing the attenuation coefficients was referred to as EMI numbers. This was then expanded by a factor of two and became known as Hounsfield units (H) where $H = \frac{\mu_{\text{tissue}} - \mu_{\text{water}}}{\mu_{\text{water}}} \times 1000$ and $\mu$ is the linear attenuation coefficient. Each Hounsfield unit is equivalent to 0.1% of the attenuation of water (*Brooks RA, Di Chiro G. 1976*) .

In addition to giving his name to the unit of attenuation, Hounsfield received many awards including the BJR Barclay prize jointly with Ambrose in 1974, the Nobel Prize for Physiology or Medicine in 1979 (Nobel lectures in physiology and medicine 1971-1980) and a Knighthood in 1981.

Hounsfield and his team created the CT scanner, which has had an explosive impact on diagnostic radiology, with little money and few resources. By the end of the 1970s they already had plans for many of the technologies which were to develop the CT scanner over the next 30 years, including helical multislice scanners and high power continuously rated scanned beam X-ray tubes.

They developed many of the techniques which formed the foundation of modern imaging including image subtraction. By 1976 the reconstruction techniques used in CT were already being applied to other areas including ultrasound and nuclear magnetic resonance.

## 2.2 CT physical principles:

### 2.2.1 Introduction:

In planar projected images of the patient, important details may be hidden by over-laying tissues. By using slice-imaging techniques (tomography), selective demonstration of morphologic properties, layer by layer, may be performed. Computerized tomography, CT, is an ideal form of tomography yielding sequence images of thin consecutive slices of the patient and providing the opportunity to localize in three dimensions. Unlike conventional, classical tomography, computerized tomography does not suffer from interference from structures in the patient outside the slice being imaged. This is achieved by irradiating only thin slices of the patient with a fan-shaped beam. Transaxial images (tomograms) of the patient's anatomy can give more selective information than conventional planar projection radiographs. Compared to planar radiography, CT images have superior contrast resolution, i.e., they are capable of distinguishing very small differences in tissue-attenuation (contrasts), but have inferior spatial resolution. An attenuation difference of 0.4% can be visualized but the smallest details in the image that can be resolved must be separated at least 0.5 mm. In conventional planar radiography, the lowest detectable contrast is larger but details of smaller size can be separated.

### 2.2.2 Principles of operation:

The formation of a CT image is a three-phase process as shown here. There are adjustable protocol factors associated with each phase that have an effect on image quality and in some cases the dose to the patient. In this

illustration we have identified so of the major protocol factors that control image quality.(www.sprawls.org)

The first phase is the scanning of the x-ray beam around and along the patient's body and the collection or acquisition of the data. This produces the scan data (but not yet an image) that is stored in the computer memory.

The second phase is the image "reconstruction" from the collected data. This results in a digital image of the individual slices or 3D volumes

The third phase is the conversion of the invisible digital image into a visible (analog) image for display and viewing. There are several adjustable factors that can be used to optimize the displayed image for a specific clinical task.

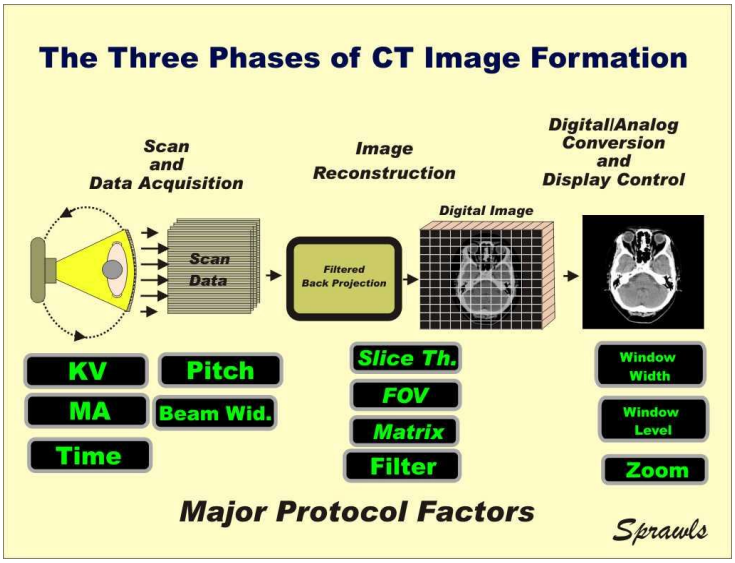


Figure 2.2.1three phases of CT image formation**(www.sprawls.org)**

### 2.2.3 The scanning motion:

In the scan phase there are two distinct motions of the x-ray beam relative to the patient's body as shown here. One is the rotation of the x-ray tube and x-ray beam around the body to produce many different "views" thought the body.

The other is scanning along the length of the patient and is achieved by moving the body thought the scanner while the beam is rotating around it.

It is the combination of these two motions that produce the complete set of data from which the images can be reconstructed.

### 2.2.4 Views and rays:

From each x-ray tube position it typically projects a thin, fan-shaped beam through the patient's body. After passing thought the body the beam in intercepted by an array of radiation detectors.

The pathway from each x-rat tube focal spot position to each detector element is designated as a ray. The detector measures the radiation that penetrates the body along each ray and records it as one data point.

As the x-ray tube is scanned around the body it produces views from each position, typically about every one degree of angle. One complete scan around the body produces several hundred views. Data from these many views are required to produce a high-quality image for each slice.

The data set to produce an image of one slice is made up of the measurement of each ray in each view. A very large quantity of data.

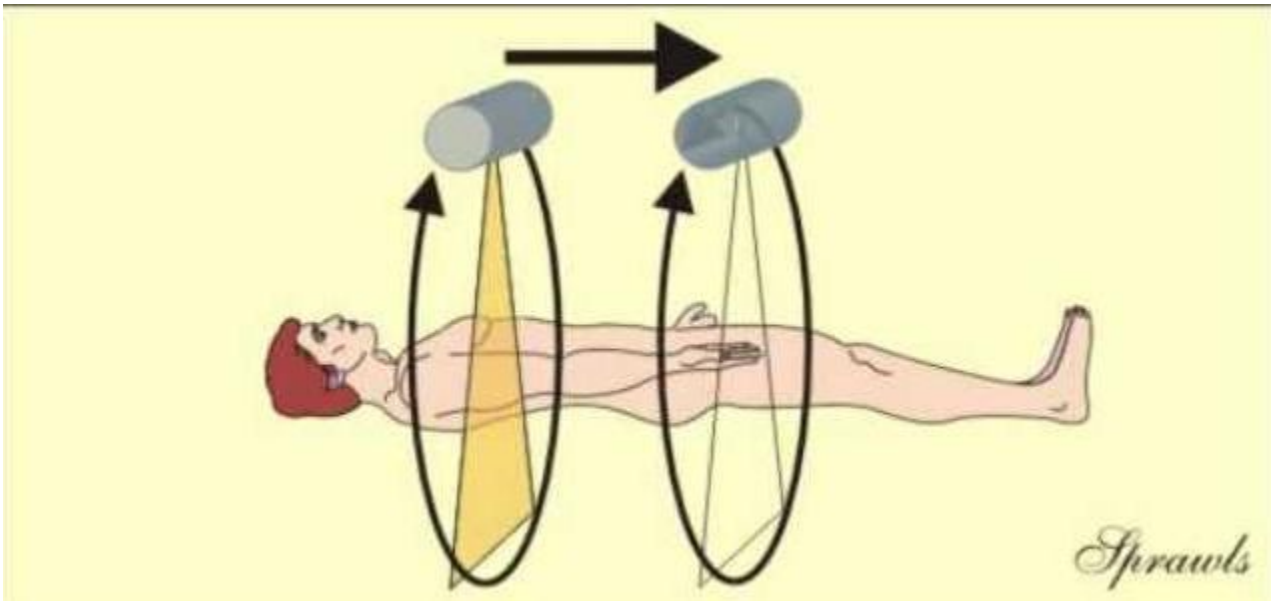


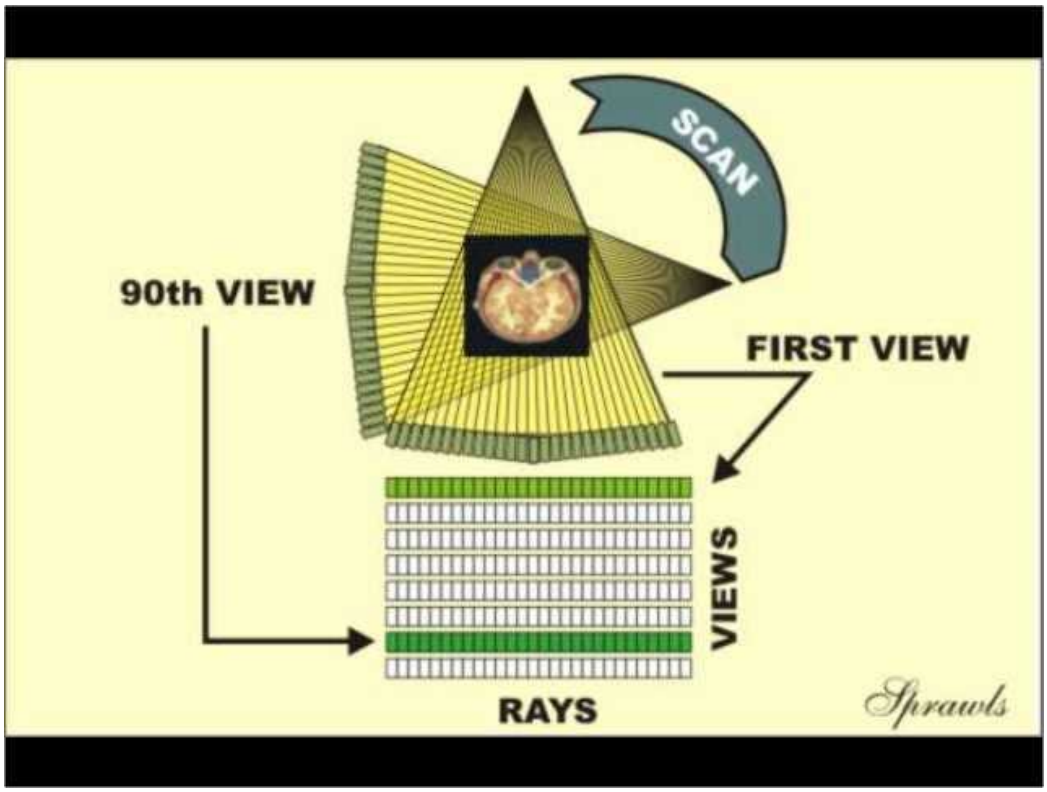


**Figure 2.2.3 CT rays and view**(www.sprawls.org)

## 2.2.5 Multiple Row Detectors:

Most CT scanners have detector arrays consisting of multiple rows compared to the single row detectors that were common in the past. The major advantage of multiple-row detectors is they produce multiple, parallel views in each tube position which increases the speed of collecting scan data along the patient's body.

A design characteristic of a scanner is the number of detector rows (16, 32, 64, etc).

A fan-beam scanner has approximately the same number of rows as number of detector elements in each row.

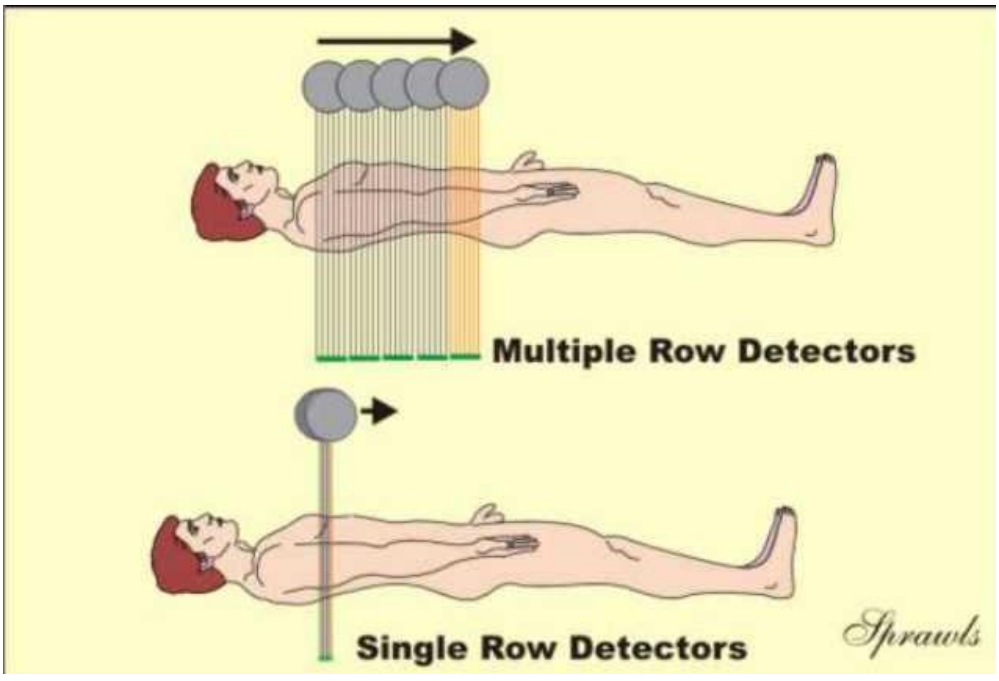


Figure 2.2.4 single and multiple row detector (www.sprawls.org)

In order to form or reconstruct an image of a specific anatomical slice or volume there must be sufficient scan data for that part of the body. There are two distinct methods of scanning the beam along the length of the body. Each has its characteristics that must be considered. (www.sprawls.org)

The simplest, and the only method available for many years is the "scan and step" method illustrated here. With the body not moving the x-ray beam is rotated completely around the body and a data set for a slice is collected. With this method the data set is "locked" to a specific slice determining its thickness and position. (www.sprawls.org)

After each beam rotation the body is then moved or "stepped" to the next slice position where it is scanned(www.sprawls.org).

The two major limitations of this method are that it is relatively slow in covering a body section and the slices (position and thickness) are fixed at the time of the scan and cannot be changed later(www.sprawls.org).

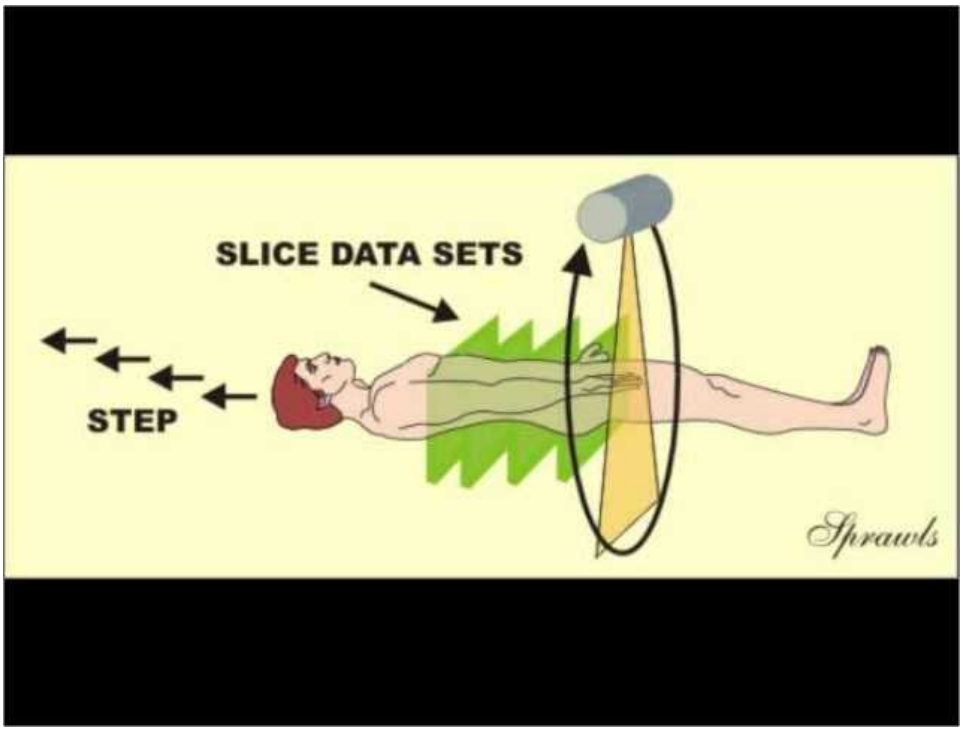


Figure2.2.5 CT scanning by step (www.sprawls.org)

## 2.2.6 Helical and Spiral Scanning:

The preferred alternative for many procedures is the helical or spiral scanning method shown here (www.sprawls.org). With this method there are two continuous motions occurring at the same time. The x-ray tube and beam is rotating around the body continuously and at the same time the body is being moved through the scanner (www.sprawls.org).

If we can imagine the path of the x-ray beam on the patient's body it would form a spiral or helical pattern. Either name is an appropriate description of this method (www.sprawls.org) .

There is one very important adjustable protocol factor associated with this method that can have an effect on both image quality and dose to the

patient. That is the Pitch factor which is the distance the body is moved, as a multiple of the beam width, during one rotation of the x-ray beam. For example, if the pitch is set to a value of 2, the body would be moved twice the thickness of the beam during on rotation (www.sprawls.org).

Increasing the pitch value increases the relative speed of moving the body and reduces the time required to cover an anatomical area. We will come back to this in more detail later but in general increasing pitch reduces the dose to the patient but can limit image quality (www.sprawls.org) .

A very significant value of spiral/helical scanning is the characteristics of the data set that is produced as illustrated here (www.sprawls.org).

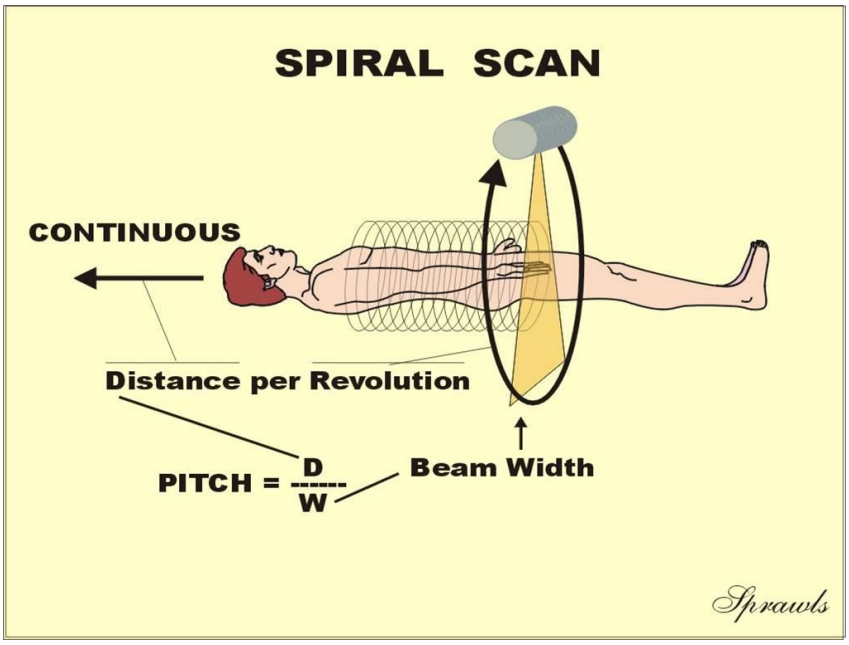


Figure2.2.6 CT spiral scanning (www.sprawls.org)

The data set is continuous over the anatomical area scanned and not divided into individual slices as with the scan and step method described above. This offers much flexibility when the images are being reconstructed. With the continuous data set it is possible to reconstruct images of slices anywhere within the data set. These images can be reconstructed for different slice thicknesses and orientations (www.sprawls.org).

With spiral scanning the slices are determined at the time of reconstruction, not at the time of the scanning and data collection. It is possible to go back and reconstruct images for different slice characteristics without scanning the patient again (www.sprawls.org).

Another great value of helical scanning is that the continuous data set can be used to reconstruct 3D or volume (compared to slice) images (www.sprawls.org).

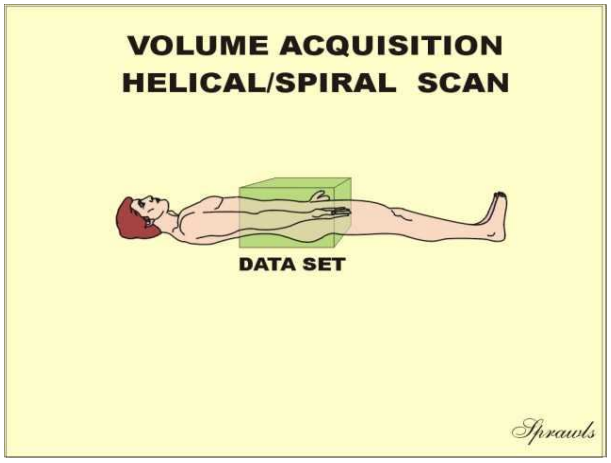


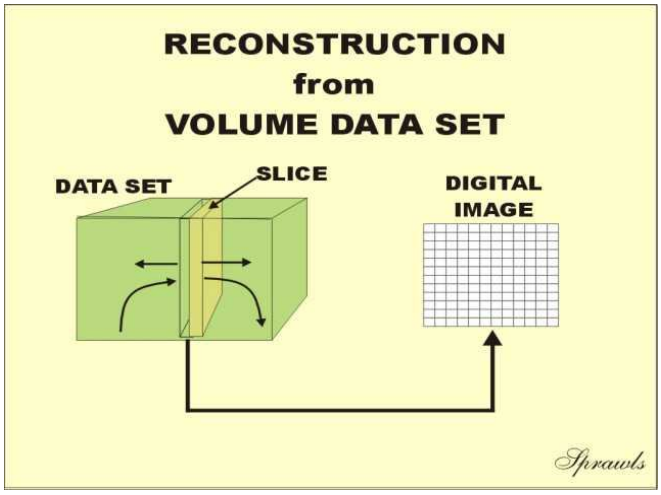


Figure2.2.7 CT volume acquisition

figure2.2.8 CT reconstruction of

(www.sprawls.org) data (www.sprawls.org)

## 2.2.7 CT Image Reconstruction and Voxels:

CT image reconstruction is a mathematical process for converting the scan data into a digital image of a specific anatomical area. Most images are created with the filtered back-projection method or sometimes with an enhanced process generally known (generically) as iterative reconstruction. It is not necessary for us to go into the mathematical details but focus on certain characteristics of the reconstruction process that are adjustable and have an effect on image quality and radiation dose (www.sprawls.org).

## 2.2.8 Voxels:

During the reconstruction process each slice is formed and divided into a matrix of voxels (volume elements) as we see here. One of the most critical factors in CT image quality and patient dose is the size of the individual voxels. The size is controlled by a combination of three protocol factors: the field of view (FOV), matrix size (number of voxels in each direction), and the slice thickness (www.sprawls.org).

The voxels in the slice of tissue are generally represented by pixels (picture elements) in the reconstructed digital image (www.sprawls.org).

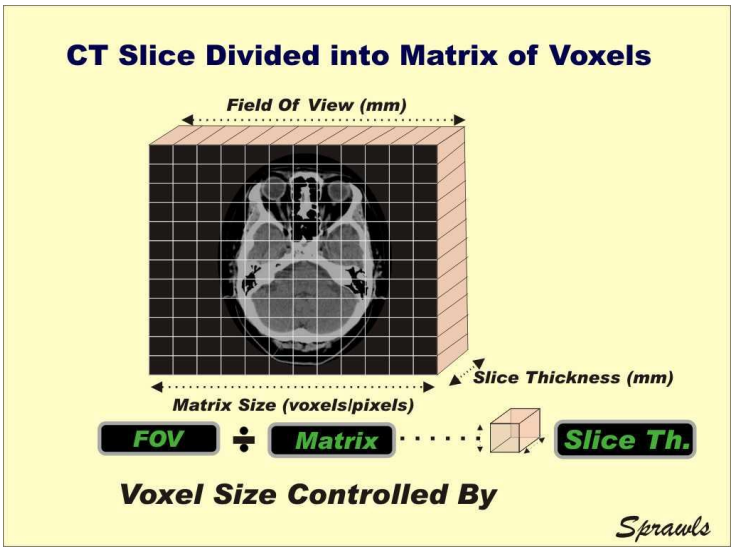


**Figure 2.2.9 CT matrix voxels** (www.sprawls.org)

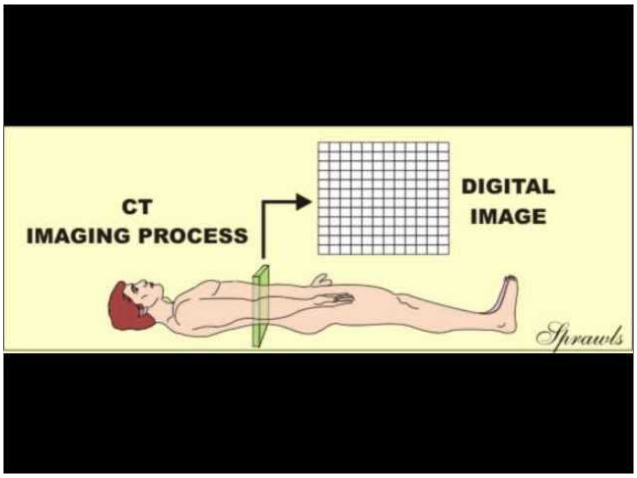


**figure 2.2.10 CT imaging process**(www.sprawls.org)

## 2.2.9 CT Numbers:

Let's continue to develop the relationship between the tissue voxels within the slice and the pixels in the image (www.sprawls.org).

Let's recall that during the scanning phase the individual rays of the x-ray beam are projected through the patient's body. They are attenuated (absorbed) in proportion to the attenuation properties of the tissue along the path. This property is represented by the value of the attenuation coefficient for the specific tissue. Because of the characteristics of the x-ray beam used in CT (high KV and heavy filtration) the attenuation is highly dependent on tissue density (www.sprawls.org).

During the back projection reconstruction process the attenuation coefficient value of each individual voxel is calculated. However, we never see the actual attenuation coefficient values because there is another step in the mathematical process performed by the computer(www.sprawls.org).

A CT number value is calculated from the attenuation coefficient value for each voxel and becomes the value for the corresponding pixel in the digital image. The formula for this calculation is shown in the illustration.

Water ($H_2O$) is used as the reference and calibration material for CT numbers. Water has the assigned CT number value of zero. Tissues or other substances that are more dense than water will have positive (+) values and those that are less dense will have negative (-) values (www.sprawls.org).

CT numbers calculated in this matter are in Hounsfield units, named for Sir Geoffrey Hounsfield, the engineer who invented and developed computed tomography (www.sprawls.org).

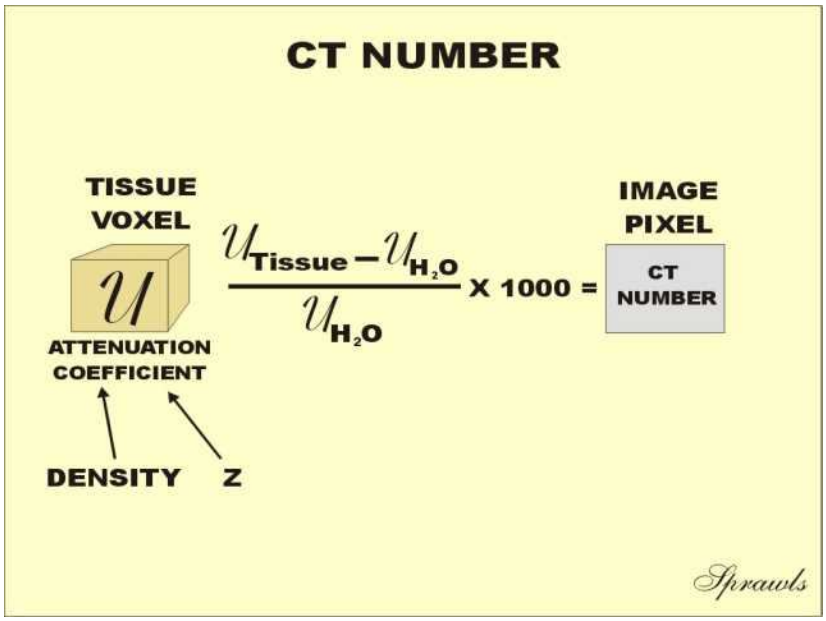


Figure2.2.11 CT number (www.sprawls.org)

## 2.2.10 Hounsfield Unit Scale:

The CT numbers in Hounsfield Units, with water at the zero (0) point, range from negative (-) 1000 for air to plus (+) approximately 3000 for dense bone (www.sprawls.org).

Since CT number values are strongly related to tissue densities the various tissues and materials are distributed along the scale according to their density. It is this difference in densities that is the source of the physical contrast that will be converted and displayed as visible contrast in the images (www.sprawls.org).

To a great extent, the very high contrast sensitivity of CT is derived from the the ability to select a small range of CT numbers and display them over the full brightness range (dark black to bright white) in the image. This occurs during the third phase of the process and can be controlled by the person viewing the image (www.sprawls.org).

The range of CT numbers to be displayed in the image is designated as the WINDOW. The two adjustable protocol factors that control the window are the LEVEL and the WIDTH (www.sprawls.org).

The LEVEL control sets the midpoint of the window range along the CT number scale. It can be used to optimize the image contrast for viewing different anatomical regions. A relative low window might be used for seeing the contrast within the lungs and a high window to see contrast within bones (www.sprawls.org).

The WIDTH setting is very much of an image contrast control. Reducing the window width increases the contrast among tissues as they are displayed in an image(www.sprawls.org).

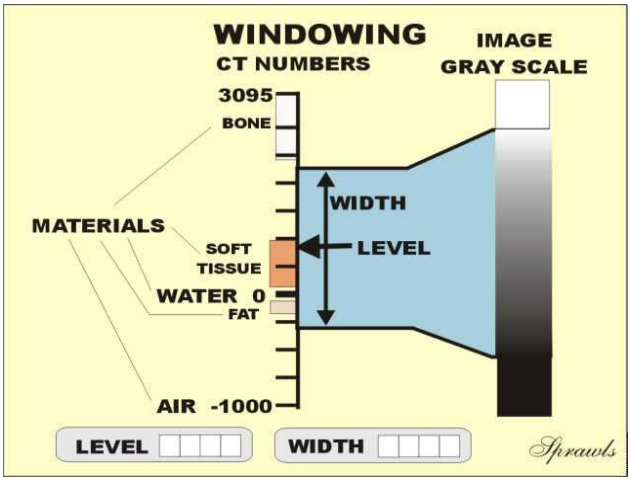


**Figure2.2.12 CT windowing** (www.sprawls.org)

### 2.2.11 Absorbed Dose:

Let's begin with a review of the concept of radiation dose. It is defined as the concentration of radiation energy absorbed in a specific tissue location within the body. The most common unit for expressing dose values is the grey (G) defined as the absorption of a joule of energy per kilogram of tissue. We emphasize that dose is the concentration of absorbed energy at each point in the body. That is, there is a dose value for every point or location within the body (www.sprawls.org).

What makes the determination and description of dose for a specific patient very difficult is that the radiation is unevenly distributed throughout the body as the x-ray beam is scanned around and along the body (www.sprawls.org).

Another quantity that is sometimes used is the total radiation energy absorbed in the body without regards to the anatomical location.

Each, absorbed dose and total radiation energy, has its place in expressing relative risks to patients (www.sprawls.org).

We will now continue developing the methods for determining the dose to a patient (www.sprawls.org).

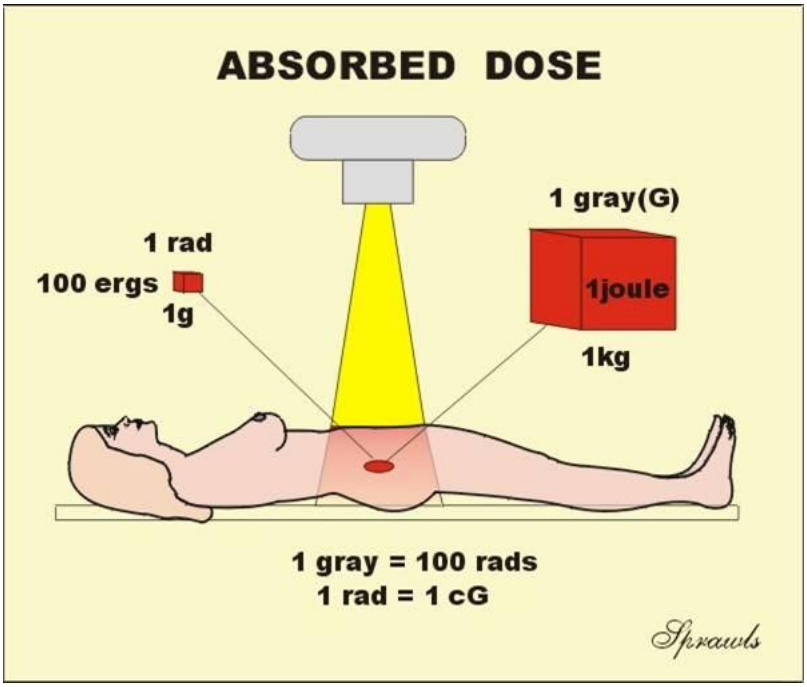


Figure2.2.13 CT absorbed dose (www.sprawls.org)

## 2.2.12 Dose Distribution within the Patient:

A major factor contributing to the complexity of determining the dose for a specific patient in the variation in distribution both within a slice and also along the length of the body (www.sprawls.org) .

Within the plane of each slice there is variation in the dose because of the shape and size of the body and internal composition. The variation can be different for heads compared to the larger sections of the body(www.sprawls.org).

In general, the dose is usually somewhat lower at the center of the body.

Now let's consider the distribution of dose along the length of the patient by looking at the dose for a single slice scan below (www.sprawls.org).

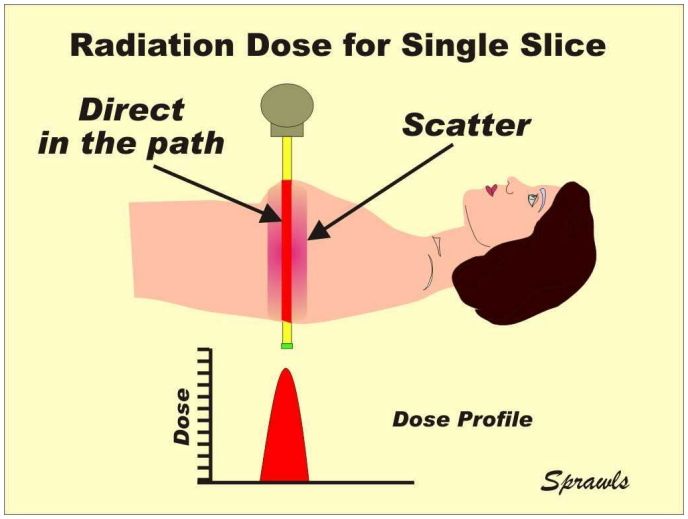


Figure2.2.14 CT radiation dose for single slice (www.sprawls.org)

Most of the dose is deposited in the slice that is being scanned but there is also some radiation that scatters out of the slice and produces some dose in the adjacent tissues (www.sprawls.org).

This scattered radiation complicated the process of determining the dose when more that one slice is imaged as in the usual procedure (www.sprawls.org).

An additional complication is the fact that we cannot place instruments, or dosimeters, directly into the body to make measurements (www.sprawls.org) .

Because of this combination of factors and challenges the dose values for a specific patient are determined or estimated through a series of external measurements and calculations (www.sprawls.org).

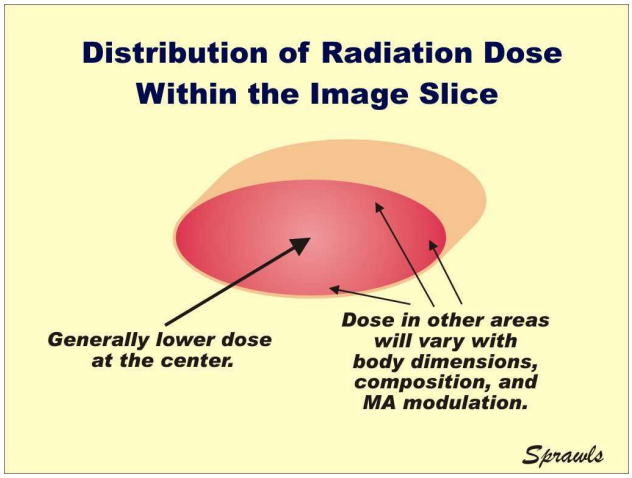


Figure 2.2.15 CT distribution of radiation dose within image slice (www.sprawls.org)

## 2.2.13 Computed Tomography Dose Index (CTDI):

Because it is not practical to measure directly the dose deposited in a patient's body an indirect, and somewhat complex process is used. We will now go thought that process which takes into account some of the variable factors that must be considered (www.sprawls.org) .

The first step is to measure the dose in a phantom that represents a patient body. The typical phantom is an acrylic cylinder that has the same x-ray absorption properties as soft tissue. It is described as being a "tissue equivalent" material with approximately the same density and effective atomic number (Z) as soft tissue (www.sprawls.org).

A smaller phantom is used to represent a head and a larger one for the abdominal section.

A dosimeter, typically an ionization chamber, is placed in the phantom and a one-slice scan is performed and the dose measured.

Now to consider the first problem. As we observed earlier some radiation scatters out of the scanned slice and exposes the adjacent tissue. This becomes significant in the typical scan which consist of many slices. The question (?) is "what is the dose within one slice" from both the direct x-ray beam through the slice and the scatter from other slices? The problem is we do not have any practical method to measure the dose in any one slice when it is within the midst of other slices that would expose the dosimeter to their direct radiation (www.sprawls.org) .

Now for the solution...it has been demonstrated that if a dose measurement is made for just one scanned slice the scattered radiation out of the slice and measured by the dosimeter will give a good approximation to the dose within a slice including the scattered radiation from adjacent multiple slices.

Since this is not an actual direct measurement, but an indirect approximation, under multiple slice conditions it cannot correctly be referred to as "dose". The value measured by this process and used as an estimate of the actual dose is described by Computed Tomography Dose Index (CTDI).

Therefore, CTDI values, and not actual dose values, are used to describe the radiation to patients (www.sprawls.org).

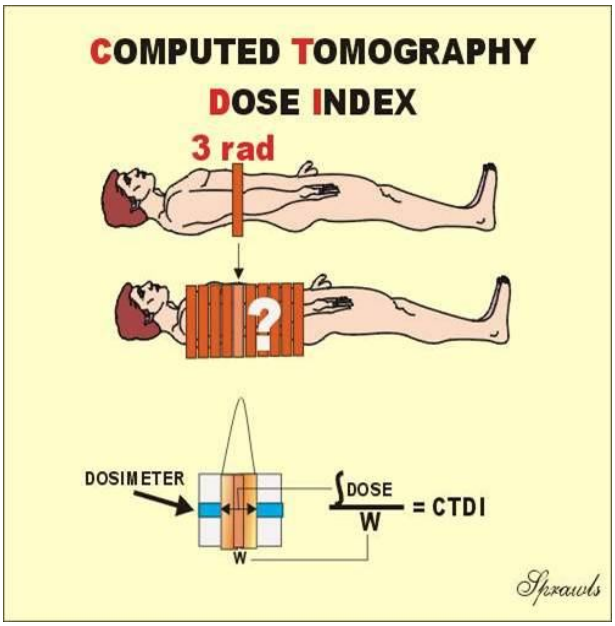


Figure 2.2.16 CTDI (www.sprawls.org)

## 2.2.14 Weighted CTDI:

As we continue with the process of determining and expressing the radiation dose to a patient the next factor to consider is the variation in dose values within the plane of a slice as described before(www.sprawls.org).

To account for this the usual procedure is to use a phantom with five (5) dosimeters. The five measured values are then used to calculate a "weighted" value using the formula shown here (www.sprawls.org).

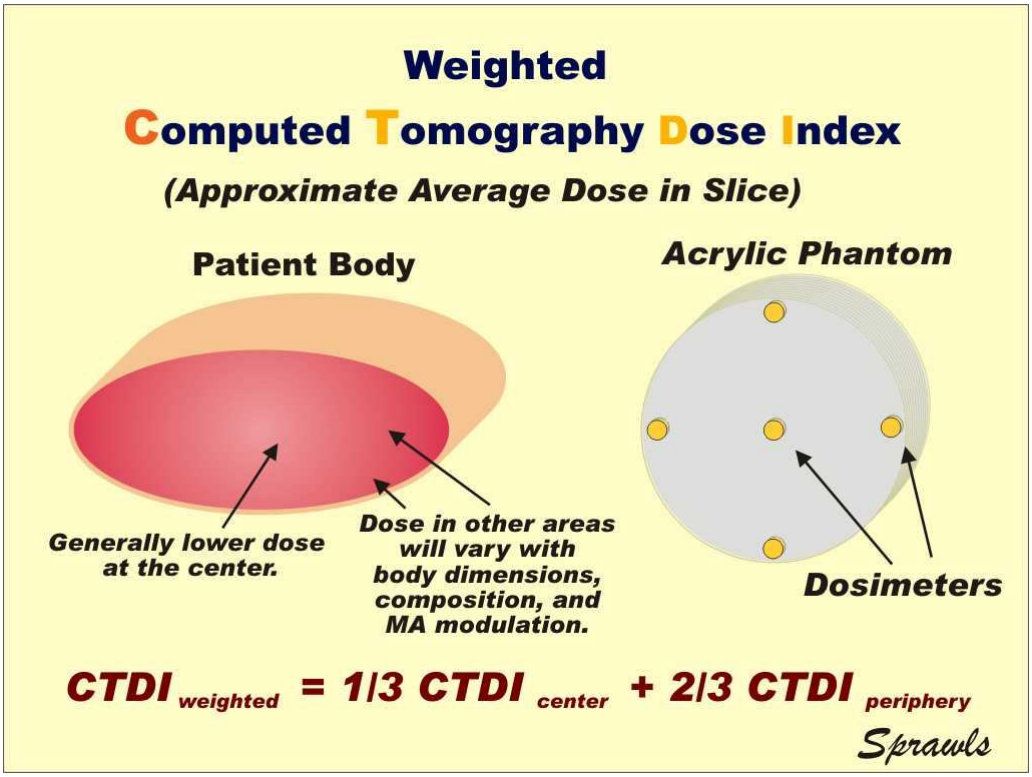

Figure 2.2.17 Weighted CTDI (www.sprawls.org)

## 2.2.15 Volume CTDI:

Now to take into account another factor, the effect of pitch on dose (www.sprawls.org).

We have already introduced the adjustable protocol factor, pitch, as having an effect on how fast the body is moved through the x-ray beam. Since dose is the concentration of radiation absorbed in tissue, increasing the pitch value with all other factors remaining unchanged "spreads" the radiation and makes it less concentrated. The dose becomes inversely proportional to the pitch.

The volume CTDI is determined by dividing the weighted CTDI by the pitch and provides an estimate of the dose for specific pitch values used in spiral scanning (www.sprawls.org).

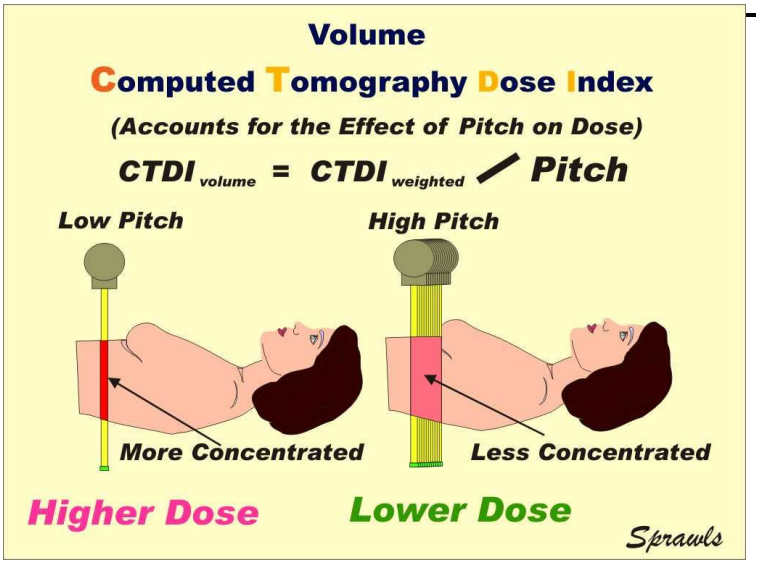


**Figure 2.2.18 Volume CTDI** (www.sprawls.org)

## 2.2.16 Radiation Dose for Multiple Slices:

The CTDI as we have developed up to this point provides an estimate of the dose within individual slices (www.sprawls.org).

The important point to remember is that "dose" is a quantity that expresses the concentration of radiation energy absorbed at a specific point within the body. Scanning multiple slices does not multiply the concentration within the individual slices, it does deposit radiation energy (dose) in additional slices (www.sprawls.org) .

With multiple slices there is some, but relatively small, increase in the dose to a slice by the scattered radiation from adjacent slices. This is probably in the range of 10% - 20%, depending on specific conditions (www.sprawls.org).

It increases the total radiation energy deposited in the body, but not the concentration in any of the slices, except for the scatter contribution (www.sprawls.org).

Our next step is to come up with a quantity that can be used to express the relative amount of total radiation to the body (www.sprawls.org).

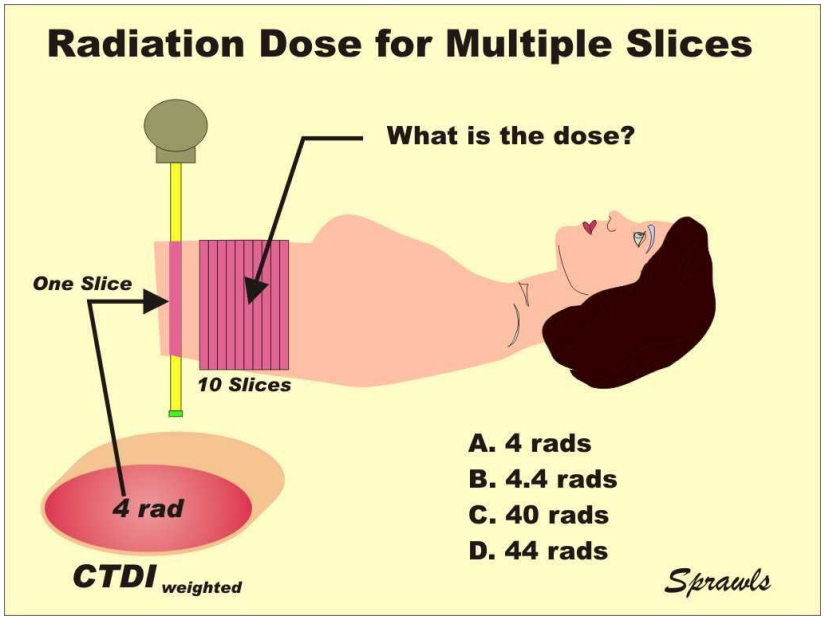


**Figure 2.2.19 CT radiation dose for multiple slices** (www.sprawls.org)

## 2.2.17 Dose Length Product (DLP):

The total radiation energy deposited in a patient's body can be estimated by multiplying the dose within a slice by the distance (length) scanned along the body as illustrated here (www.sprawls.org).

The advantage of DLP is that it is relatively easy to determine for each patient scan. Many scanners can automatically calculate it and display the value as part of the patient information(www.sprawls.org).

There are two ways that DLP values can be used.

They can be used to compare various scanning protocols with respect to the total energy imparted to a patient. Since this is not an actual energy unit it provides a relative comparison only(www.sprawls.org).

DLP values when combined with other factors can be used to calculate the effective dose to the patient (www.sprawls.org).

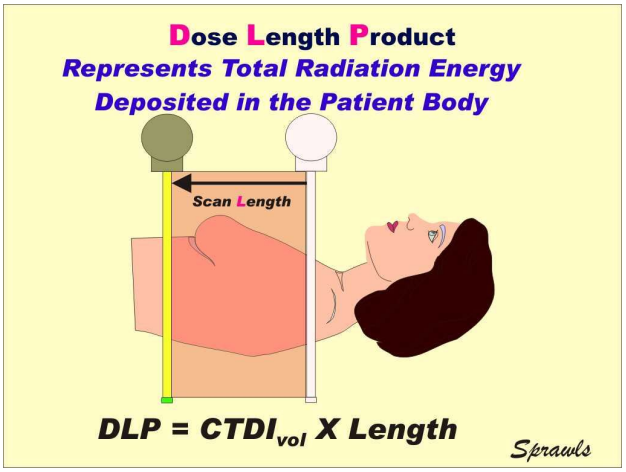


**Figure 2.2.20 CT DLP** (www.sprawls.org)

## 2.2.18 Effective Dose:

First, a quick review. Let's recall that effective dose is the quantity that is used to estimate relative risk to a patient taking into account the distribution of dose values to the various organs and anatomical regions and the relative sensitivity of the different tissues as quantified in terms of the values for the tissue weighting factors (www.sprawls.org).

The value calculated for effective dose is generally assumed to have the same detrimental biological effect as a dose of that value to the whole body(www.sprawls.org).

The effective dose for a CT scan can be calculated from a DLP value using tabulated data of the tissue weighting factors for the organs within the scanned area (www.sprawls.org).

Effective dose values are generally used to compare the relative risks of various CT imaging protocols (www.sprawls.org).

Also, effective dose values are used to compare a CT procedure to normal background radiation which is a whole-body exposure (www.sprawls.org).

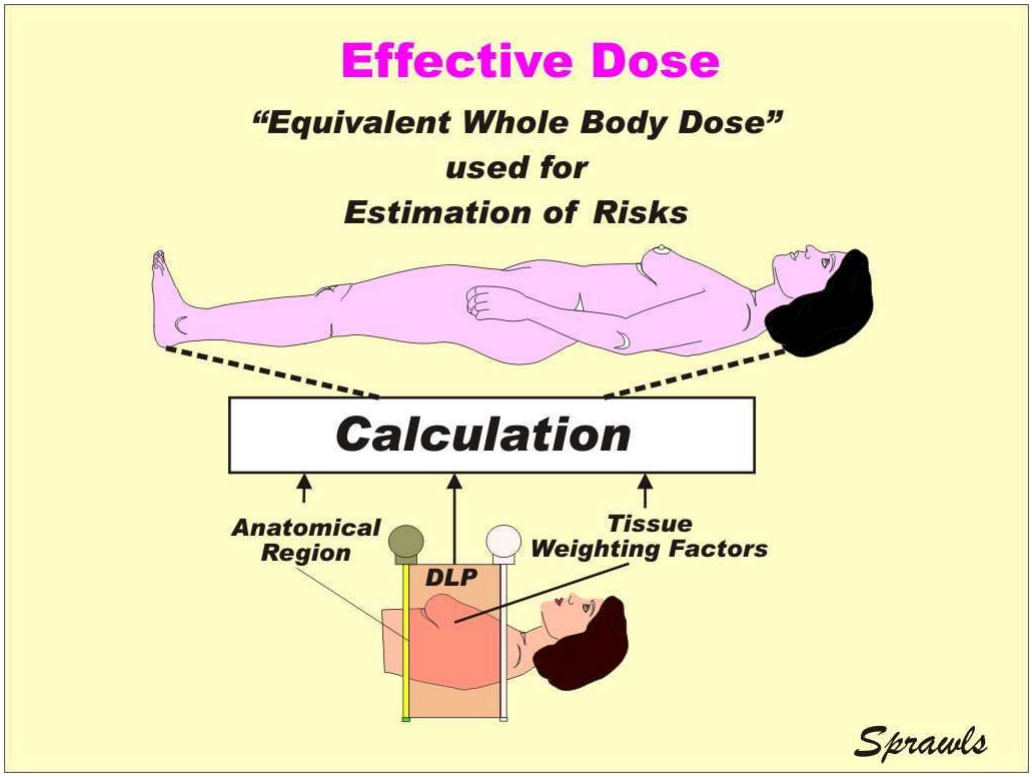


**Figure 2.2.21 Equivalent dose** (www.sprawls.org)

## 2.2.19 CT Dose Quantities:

We are almost there! Our goal is to determine a dose value for a patient undergoing a CT procedure. As we have observed, there are a variety of factors that must be considered and several different quantities associated with the factors and conditions (www.sprawls.org).

The first step, usually performed by a physicist, is to measure the weighted CTDI in a phantom. This provides basic calibration data for the scanner (www.sprawls.org).

By using the KV, Time, and MA values for a specific patient and the calibration data the weighted CTDI for the patient can be calculated (www.sprawls.org).

The next step is to use the pitch value (spiral/helical scanning) to calculate the volume CTDI. This is often calculated and displayed by the scanner as part of the patient information (www.sprawls.org).

Multiplying by the length of the scan provides a value for the DLP, the relative total energy imparted to the body. This is also calculated and displayed by many scanners (www.sprawls.org).

The final step is the calculation of the effective dose that provides an estimate of the relative biological effect on the patient (www.sprawls.org).

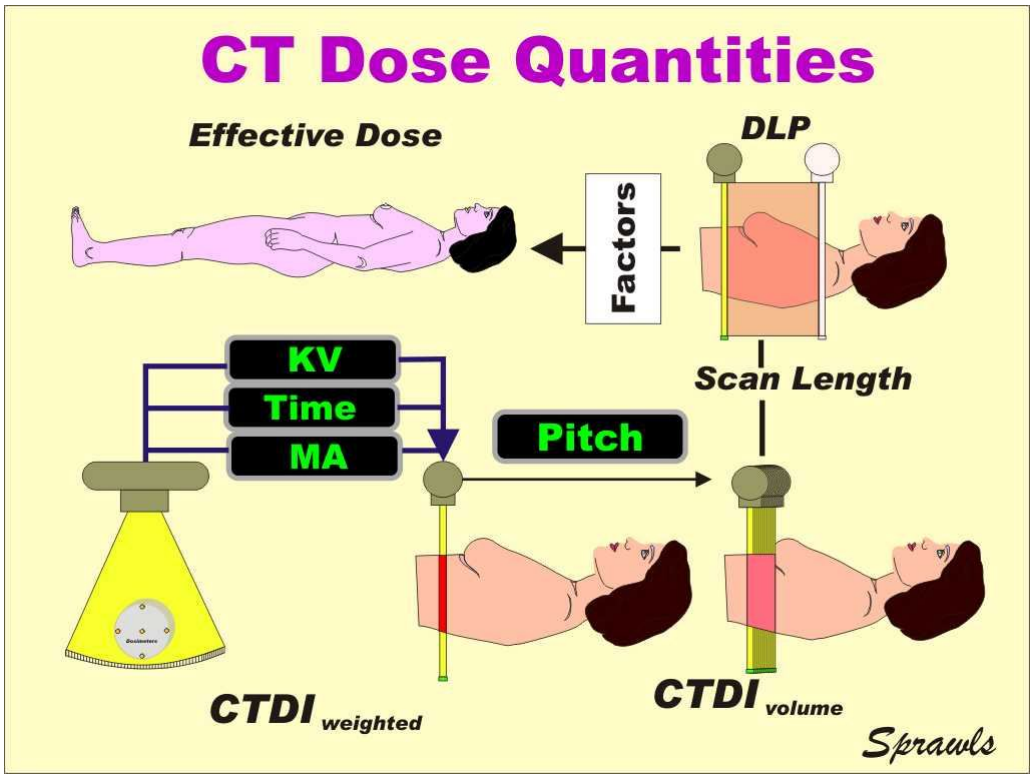


figure 2.2.22 CT dose quantities (www.sprawls.org)

## 2.2.20 Image quality:

The one comprehensive CT image quality characteristic is visibility(www.sprawls.org). That is the visibility of anatomical structures, various tissues, and signs of pathology. However, visibility depends on a somewhat complex combination of the five (5) more specific image characteristics shown here(www.sprawls.org). Let's go ahead and introduce them by name:

**Contrast Sensitivity.**

**Visibility of Detail**, as affected by blurring (Sometimes called spatial resolution).

**Visual Noise.**

**Artifacts.**

**Spatial** or geometric characteristics of the image/body relationship.

Each of these can have an effect on the **visibility** of specific anatomical or pathologic objects within the body (www.sprawls.org).

Now the important point is that each of these characteristics is generally adjustable and can be changed or set by a combination of the protocol factors. The challenge is it is not a "one-to-one" relationship. One protocol factor (such as slice thickness) has an effect on both detail and noise (www.sprawls.org).

It is this complex combination of protocol factors that will make up an optimized procedure that we will now be working on (www.sprawls.org).

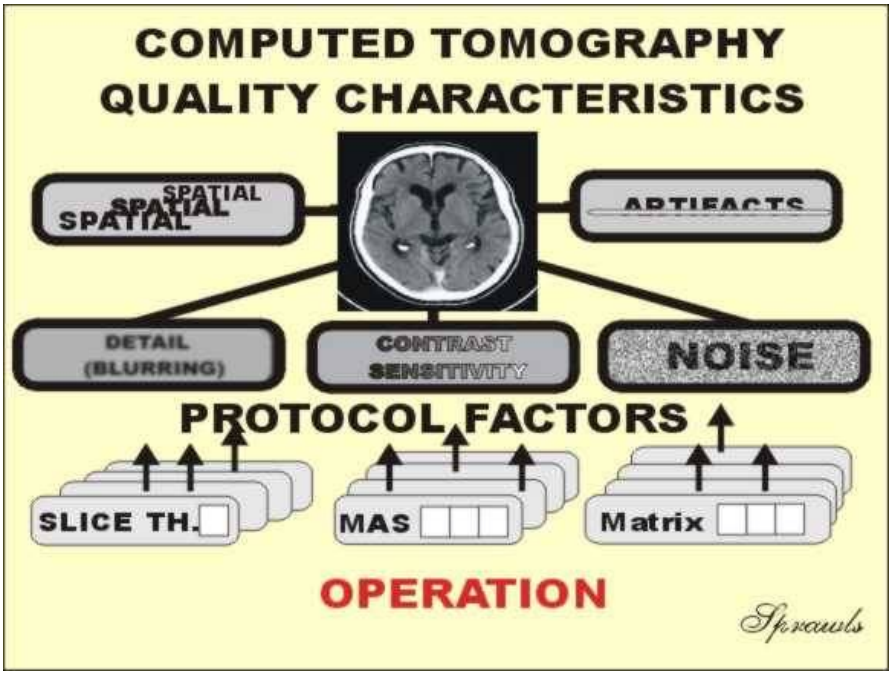


Figure 2.2.23 CT quality characteristic (www.sprawls.org)

### 2.2.20.1 Contrast Sensitivity:

All of the image characteristics are important and have a potential effect on visibility but the characteristic, contrast sensitivity, is especially significant in CT because it is what makes it a superior imaging modality for many clinical procedures. The concept of contrast sensitivity is illustrated here. Contrast sensitivity is a characteristic of the imaging process. That is the capabilities of the imaging equipment (CT scanner) and how it is adjusted. Contrast sensitivity controls the conversion of the physical contrast within the body to the visible contrast in an image (www.sprawls.org).

With CT imaging the principle source of physical contrast within a body are the differences in physical density among the tissues. An exception is when an

iodine-based contrast medium is used where it becomes more of an atomic number (Z) effect (www.sprawls.org).

Compared to other x-ray imaging modalities CT has a very high contrast sensitivity for "seeing" the soft tissues and differences among the tissues in the body. How this is produced and controlled will be illustrated later (www.sprawls.org).

Within a body there will be tissues and objects with a range of densities and physical contrast. As illustrated here things like bones, bullets, and barium have a very high physical contrast relative to the soft tissues. Imaging them is not a problem. The real challenge is imaging the very low density differences between and among the soft tissues (www.sprawls.org).

Contrast sensitivity determines the range of visibility with respect to physical contrast (www.sprawls.org). If a procedure has low contrast sensitivity then only objects with high physical contrast will be visible (www.sprawls.org).

When a procedure, such as CT, has high contrast sensitivity then tissues with small differences in density will be visualized (www.sprawls.org).

If the contrast sensitivity is low, either because of limitations of the specific imaging modality or the adjustments of the imaging protocol factors then tissues that have small differences in density (physical contrast) will not be visible(www.sprawls.org) .

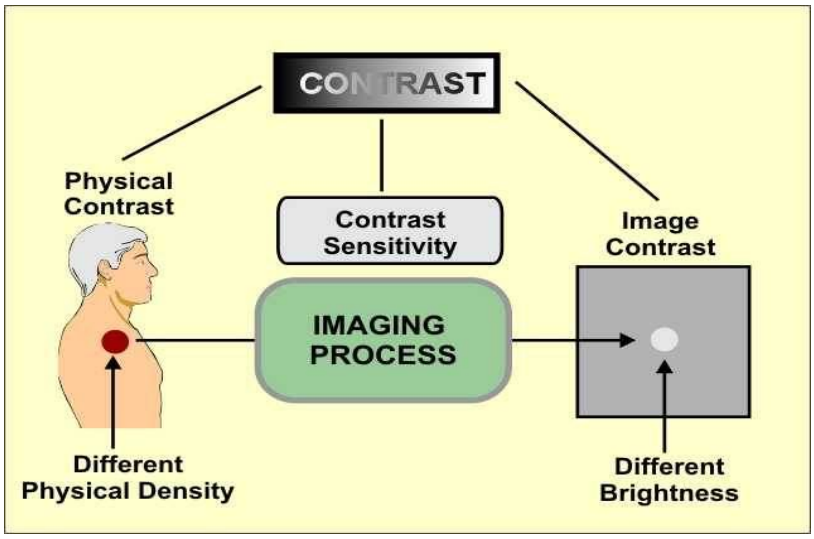


Figure 2.2.24 CT image contrast (www.sprawls.org)

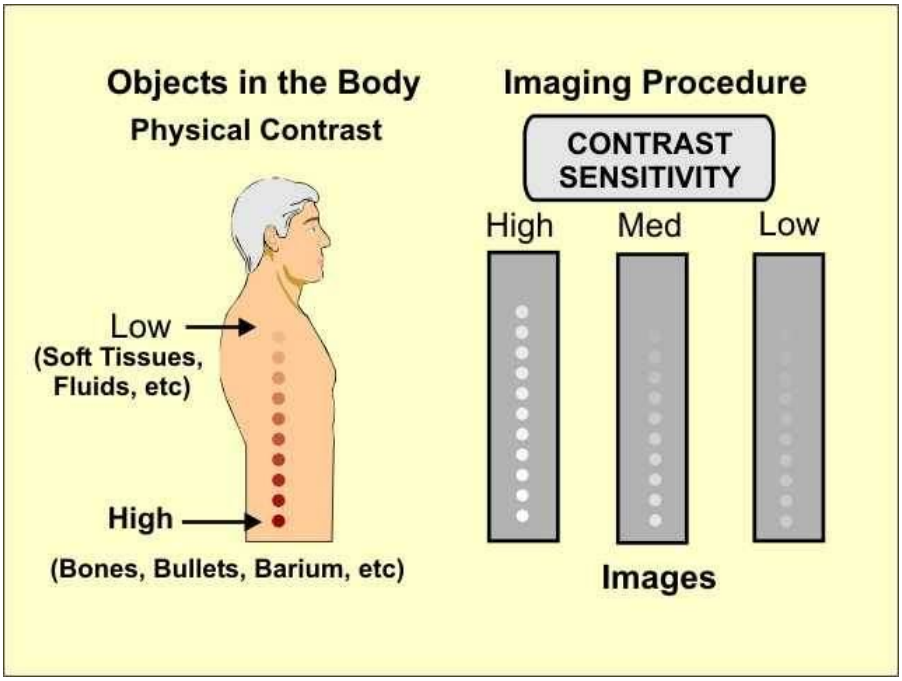


Figure 2.2.25 CT image contrast sensitivity (www.sprawls.org)

### 2.2.20.2 Visibility of Detail

A characteristic of all imaging methods, including human vision, is that there is some blurring that occurs within the process. The effect of this blurring is that it reduces visibility of detail (small objects and features). When we have blurred vision we can't read the fine print. Each medical imaging method has inherent sources of blurring that limits visibility of detail and determines the types of diagnostic procedures it can be used for(www.sprawls.org). For example, radiography which has relatively low blur and provides high visibility of detail is used for visualizing small bone fractures (www.sprawls.org).

The general relationship of detail to the blurring within the imaging process is illustrated here (www.sprawls.org).

As the blurring increases more and more of the small objects become invisible.

In the CT imaging process there are several sources of blurring that collectively limit visibility of detail (www.sprawls.org) .

There are adjustable protocol factors associated with each of these sources of blur as we will soon see (www.sprawls.org) .

The problem is when we reduce the blurring it increases another undesirable image characteristic, visual noise, and can also lead to increased radiation dose to the patient(www.sprawls.org) .

That is why we must have optimized imaging protocols that take all of these factors into account and provide a proper balance (www.sprawls.org).

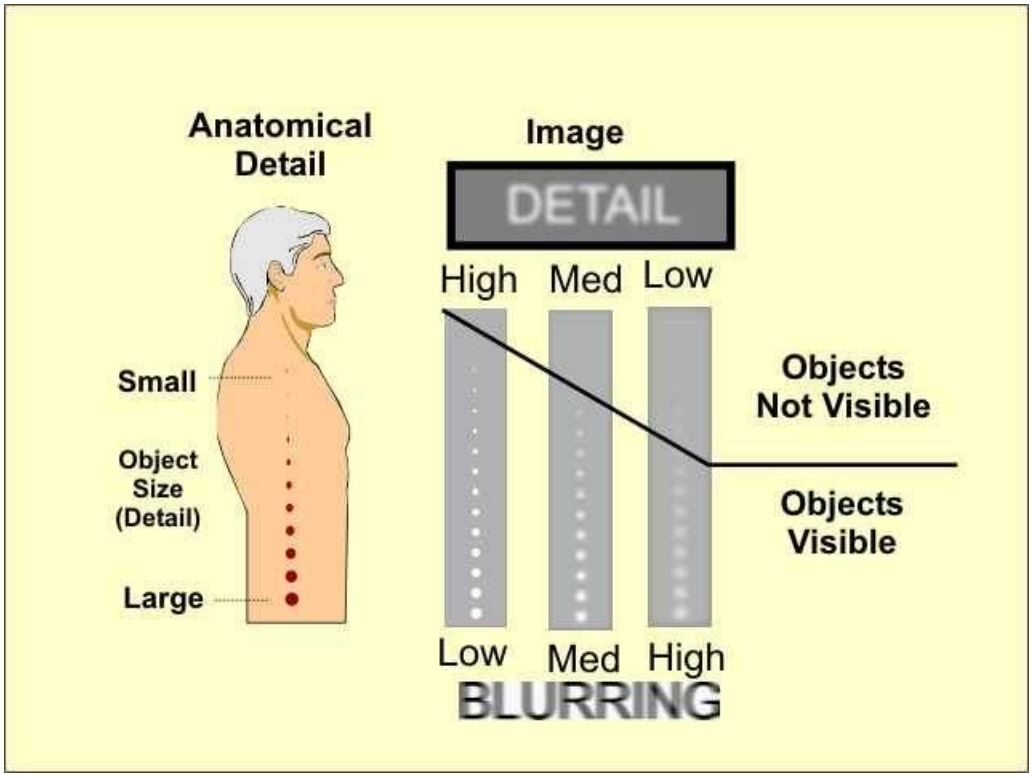


Figure2.2.26 CT image detail(www.sprawls.org)

### 2.2.20.3 Visual Noise:

All medical imaging methods produce images with some visual noise. This is generally an undesirable characteristic that reduces visibility of certain types of objects and structures as illustrated here (www.sprawls.org).

Specifically, noise reduces the visibility of low-contrast objects. This is especially significant in CT which is often used to image low-contrast differences among tissues (www.sprawls.org).

Let's take a moment to distinguish between noise and blurring. Both are characteristics that reduce visibility, but of different types of objects. Noise

reduces visibility of low-contrast objects, blurring reduces visibility of small objects or detail (www.sprawls.org).

The noise in a CT image can be adjusted with a combination of protocol factors(www.sprawls.org).

The challenge is that the factors that can be used to adjust and reduce noise also have an effect on either image detail (blurring) or radiation dose to the patient(www.sprawls.org).

That is why we must have optimized imaging protocols that take all of these factors into account and provide a proper balance(www.sprawls.org).

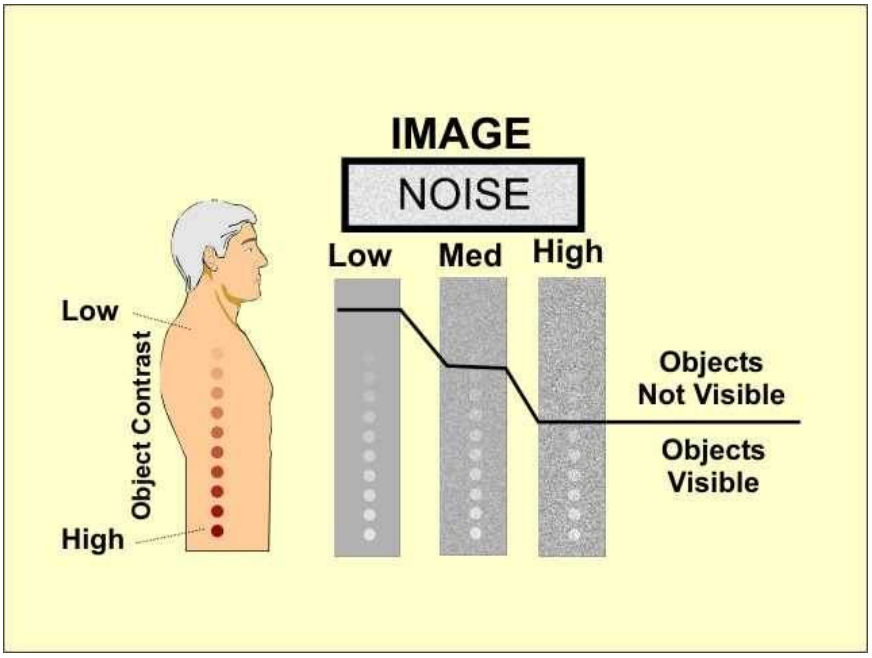


figure 2.2.27 CT image noise (www.sprawls.org)

## 2.2.20.4 Spatial and Geometric Characteristics:

The spatial and geometric characteristics of a CT image play a major role in optimizing the imaging protocols. That is because the CT image is made up of many small elements or voxels as illustrated here. The typical CT image is of a slice through the body. During the image reconstruction phase the slice is divided into a matrix of voxels (www.sprawls.org) .

It is the size of the voxels that has a major impact on image blurring, noise, and on radiation dose to the patient (www.sprawls.org).

The size of the voxels is controlled by a combination of the three protocol factors shown here.

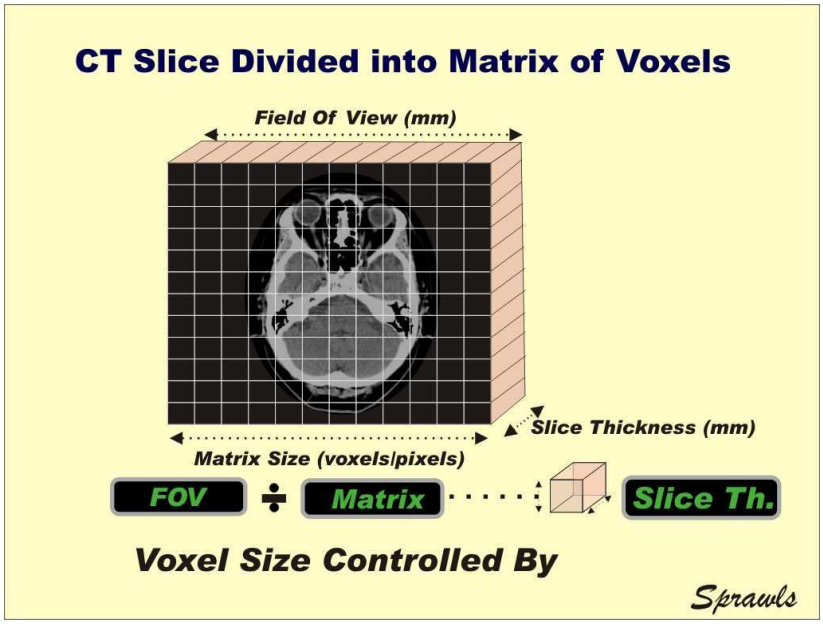


**Figure 2.2.28 CT slices divided in to matrix voxels** (www.sprawls.org)

## 2.2.20.5 Artifacts:

We finish our introduction to the five CT image characteristics with artifacts. Some possible CT artifacts are shown here. An artifact is generally something that appears in an image that is not a direct visualization of an object or structure in the body (www.sprawls.org).

There are quite a few possible artifacts coming from a variety of conditions that can occur during an imaging procedure. Some are very obvious such as streaks and "ghosts" while others are less visible but more in the form of changes in how certain areas or objects are displayed (www.sprawls.org).

With the advances in CT technology many artifacts are less common. The most effective approach to learning CT artifacts is through their observation and analysis while viewing clinical images (www.sprawls.org).

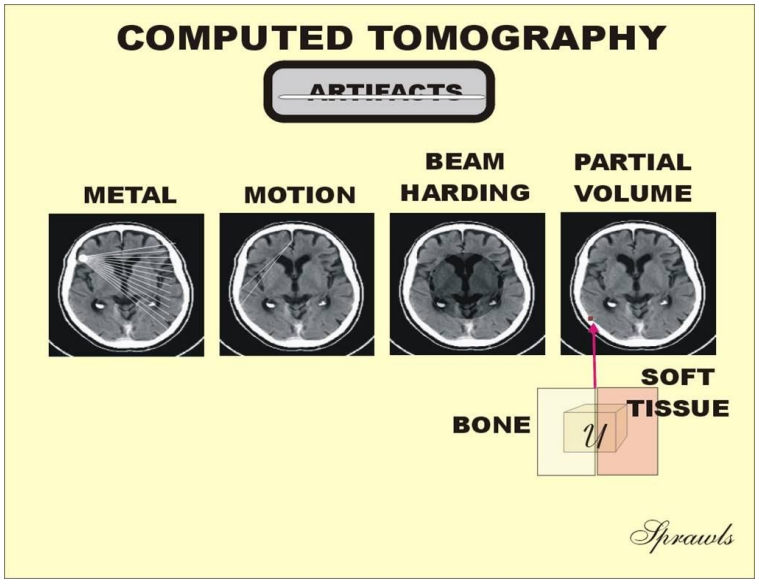


Figure 2.2.29 CT artifacts (www.sprawls.org)

## 2.3 Radiation Doses from CT Scans:

### 2.3.1 Quantitative Measures:

Various measures are used to describe the radiation dose delivered by CT scanning, the most relevant being absorbed dose, effective dose, and CT dose index (or CTDI).

The absorbed dose is the energy absorbed per unit of mass and is measured in grays (Gy). One gray equals 1 joule of radiation energy absorbed per kilogram. The organ dose (or the distribution of dose in the organ) will largely determine the level of risk to that organ from the radiation.

The effective dose, expressed in sieverts (Sv), is used for dose distributions that are not homogeneous (which is always the case with CT); it is designed to be proportional to a generic estimate of the overall harm to the patient caused by the radiation exposure. The effective dose allows for a rough comparison between different CT scenarios but provides only an approximate estimate of the true risk. For risk estimation, the organ dose is the preferred quantity.

Organ doses can be calculated or measured in anthropomorphic phantoms(Groves AM,2004). Historically, CT doses have generally been (and still are) measured for a single slice in standard cylindrical acrylic phantoms17; the resulting quantity, the CT dose index, although useful for quality control, is not directly related to the organ dose or risk( Brenner DJ 2006).

### 2.3.2 Typical Organ Doses:

Organ doses from CT scanning are considerably larger than those from corresponding conventional radiography (Table 1). For example, a conventional anterior–posterior abdominal x-ray examination results in a

dose to the stomach of approximately 0.25 mGy, which is at least 50 times smaller than the corresponding stomach dose from an abdominal CT scan.

Representative calculated organ doses for frequently used machine settings1 are shown in Figure 3A and 3B for a single CT scan of the head and of the abdomen, the two most common types of CT scan. The number of scans in a given study is, of course, an important factor in determining the

dose. For example, Mettler Et Al. reported that in virtually all patients undergoing CT of the abdomen or pelvis, more than one scan was obtained on the same day; among all patients undergoing CT, the authors reported that at least three scans were obtained in 30% of patients, more than five scans in 7%, and nine or more scans in 4%( Mettler FA Jr, Wiest PW, Locken JA, Kelsey CA 2000).

The radiation doses to particular organs from any given CT study depend on a number of factors. The most important are the number of scans, the tube current and scanning time in milliamp seconds (mAs), the size of the patient, the axial scan range, the scan pitch (the degree of overlap between adjacent CT slices), the tube voltage in the kilovolt peaks (kVp), and the specific design of the scanner being used (McNitt-Gray MF 2002). Many of these factors are under the control of the radiologist or radiology technician. Ideally, they should be tailored to the type of study being performed and to the size of the particular patient, a practice that is increasing but is by no means universal(Paterson A, Frush DP, Donnelly LF 2001). It is always the case that the relative noise in CT images will increase as the radiation dose decreases, which means that there will always be a tradeoff between the need for low-noise images and the desirability of using low doses of radiation(Martin CJ, Sutton DG, Sharp PF 1999).

| Study type | Relevant organ | Relevant organ dose (mGy or mSv) |
|---|---|---|
| Dental radiography | Brain | 0.005 |
| Posterior-anterior chest radiograph | Lung | 0.01 |
| Lateral chest radiography | Lung | 0.15 |
| Screening mammography | Breast | 3 |
| Adult abdominal CT | Stomach | 10 |
| Barium enema | Colon | 15 |
| Neonatal abdominal CT | Stomach | 20 |

**Table 2.3.1 typical organ radiation doses from various radiological studies ( www.nejm.org )**

## 2.3.3 Biologic Effects of Low Doses of Ionizing radiation:

### 2.3.3.1 Mechanism of Biologic Damage:

Ionizing radiation, such as x-rays, is uniquely energetic enough to overcome the binding energy of the electrons orbiting atoms and molecules; thus, these radiations can knock electrons out of their orbits, thereby creating ions. In biologic material exposed to x-rays, the most common scenario is the creation of hydroxyl radicals from x-ray interactions with water molecules; these radicals in turn interact with nearby DNA to cause strand breaks or base damage. X-rays can also ionize DNA directly. Most radiation-induced damage is rapidly repaired by various systems within the cell, but DNA double-strand breaks are less easily repaired, and occasional disrepair can lead to induction of point mutations, chromosomal translocations, and gene fusions, all of which are linked to the induction of cancer (Mitelman F, Johansson B, Mertens FE 2007).

### 2.3.3.2Risks Associated with Low Doses of Radiation:

Depending on the machine settings, the organ being studied typically receives a radiation dose in the range of 15 millisieverts (mSv) (in an adult) to 30 mSv (in a neonate) for a single CT scan, with an average of two to three CT scans per study. At these doses, as reviewed elsewhere,( Brenner DJ, Doll R, Goodhead DT, et al 2003) the most likely (though small) risk is for radiation-induced carcinogenesis.

Most of the quantitative information that we have regarding the risks of radiation-induced cancer comes from studies of survivors of the atomic bombs dropped on Japan in 1945(BEIR VII.

National Academies Press, 2005Washington, DC). Data from cohorts of these survivors are generally used as the basis for predicting radiation-related risks in a population because the cohorts are large and have been intensively studied over a period of many decades, they were not selected for disease, all age groups are covered, and a substantial sub cohort of about 25,000 survivors(Preston DL, Pierce DA, Shimizu Y, et 2004)received radiation doses similar to those of concern here — that is, less than 50 mSv. Of course, the survivors of the atomic bombs were exposed to a fairly uniform dose of radiation throughout the body, whereas CT involves highly nonuniform exposure, but there is little evidence that the risks for a specific organ are substantially influenced by exposure of other organs to radiation.

There was a significant increase in the overall risk of cancer in the subgroup of atomic-bomb survivors who received low doses of radiation, ranging from 5 to 150 mSv(Preston DL, Shimizu Y, Pierce DA, Suyama A, Mabuchi K Radiat Res 2003, Pierce DA, Preston DL Radiat Res 2000, Preston DL, Ron E, Tokuoka S, et al Radiat Res 2007) the mean dose in this subgroup was about 40 mSv, which approximates the relevant organ dose from a typical CT study involving two or three sans in an adult.

Although most of the quantitative estimates of the radiation-induced cancer risk are derived from analyses of atomic-bomb survivors, there are other supporting studies, including a recent large-scale study of 400,000 radiation workers in the nuclear industry(Cardis E, Vrijheid M, Blettner M, et al Radiat Res 2007, Idem. Risk of cancer after low doses of ionising radiation BMJ 2005 ) who were exposed to an average dose of approximately 20 mSv

(a typical organ dose from a single CT scan for an adult). A significant association was reported between the radiation dose and mortality from cancer in this cohort (with a significant increase in the risk of cancer among workers who received doses between 5 and 150 mSv); the risks were quantitatively consistent with those reported for atomic bomb survivors.

The situation is even clearer for children, who are at greater risk than adults from a given dose of radiation (Fig. 2.3.3), both because they are inherently more radiosensitive and because they have more remaining years of life during which a radiation-induced cancer could develop.

In summary, there is direct evidence from epidemiologic studies that the organ doses corresponding to a common CT study (two or three scans, resulting in a dose in the range of 30 to 90 mSv) result in an increased risk of cancer. The evidence is reasonably convincing for adults and very convincing for children.

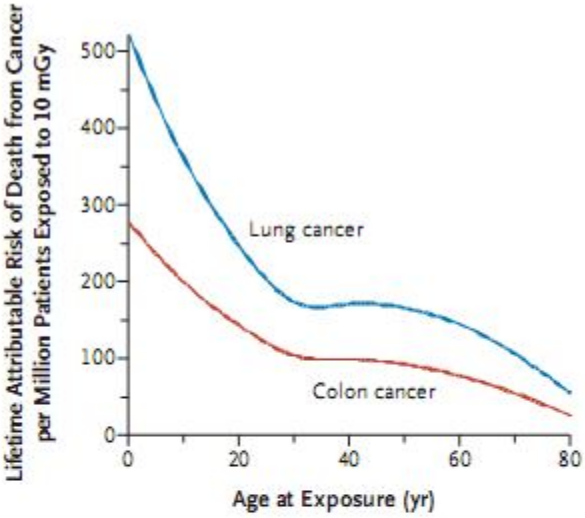


Fig. 2.3.1 **Estimated Dependence of Lifetime Radiation-Induced Risk of Cancer on Age at Exposure for Two of the Most Common Radiogenic Cancers.**

Cancer risks decrease with increasing age both because children have more years of life during which a potential cancer can be expressed (latency periods for solid tumors are typically decades) and because growing children are inherently more radiosensitive, since they have a larger proportion of dividing cells. These risk estimates, applicable to a Western population, are from a 2005 report by the National Academy of Sciences[25] and are ultimately derived from studies of the survivors of the atomic bombings. The data have been averaged according to sex. www.najm.org

### 2.3.3.3 Cancer Risks Associated with CT Scans:

No large-scale epidemiologic studies of the cancer risks associated with CT scans have been reported; one such study is just beginning(Giles J Nature 2004; ). Although the results of such studies will not be available for some years, it is possible to estimate the cancer risks associated with the radiation exposure from any given CT scan20 by estimating the organ doses involved and applying organ specific cancer incidence or mortality data that were derived from studies of atomic-bomb survivors. As discussed above, the organ doses for a typical CT study involving two or three scans are in the range in which there is direct evidence of a statistically significant increase in the risk of cancer, and the corresponding CT-related risks can thus be directly assessed from epidemiologic data, without the need to extrapolate measured risks to lower doses(Brenner DJ, Elliston CD, Hall EJ, Berdon WE 2002).

The estimated lifetime risk of death from cancer that is attributable to a single “generic” CT scan of the head or abdomen (Fig. 2.3.2C and 3D) is calculated by summing the estimated organ-specific
cancer risks. These risk estimates are based on the organ doses shown in Figure 2.3.2 A and 3B, which were derived for average CT machine settings.1

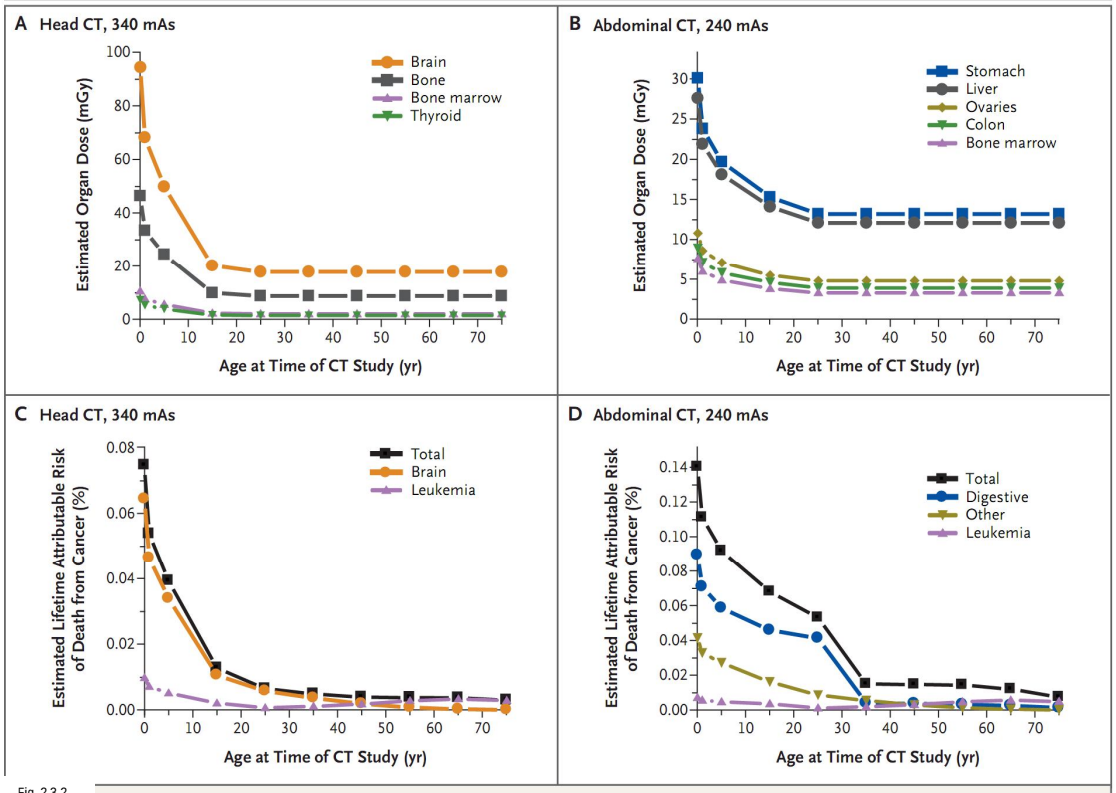


Fig. 2.3.2

**Estimated Organ Doses and Lifetime Cancer Risks from Typical Single CT Scans of the Head and the Abdomen.**

Panels A and B show estimated typical radiation doses for selected organs from a single typical CT scan of the head or the abdomen. As expected, the brain receives the largest dose during CT of the head and the digestive organs receive the largest dose during CT of the abdomen. These doses depend on a variety of factors, including the number of scans (data shown are for a single scan) and the milliamp-seconds (mAs) setting. The data shown here refer to the median mAs settings reported in the 2000 NEXT survey of CT use.[1] For a given mAs setting, pediatric doses are much larger than adult doses, because a child's thinner torso provides less shielding of organs from the radiation exposure. The mAs setting can be reduced for children (but is often not reduced[5,19]); a reduction in the mAs setting proportionately reduces the dose and the risk. The methods used to obtain these dose estimates have been described elsewhere,[20] but software that estimates organ doses for specific ages and CT settings is now generally available.[21] Panels C and D show the corresponding estimated lifetime percent risk of death from cancer that is attributable to the radiation from a single CT scan; the risks (both for selected individual organs and overall) have been averaged for male and female patients. The methods used to obtain these risk estimates have been described elsewhere.[20] The risks are highly dependent on age because both the doses (Panels A and B) and the risks per unit dose are age-dependent. Even though doses are higher for head scans, the risks are higher for abdominal scans because the digestive organs are more sensitive than the brain to radiation-induced cancer. www.najm.org

Although the individual risk estimates shown in Figure 2.3.2 are small, the concern about the risks from CT is related to the rapid increase in its use —small individual risks applied to an increasingly large population may create a public health issue some years in the future. On the basis of such risk estimates and data on CT use from 1991 through 1996, it has been estimated that about 0.4% of all cancers in the United States may be attributable to the radiation from CT studies.2,34 By adjusting this estimate for current CT use

(Fig. 2.3.1), this estimate might now be in the range of 1.5 to 2.0%.

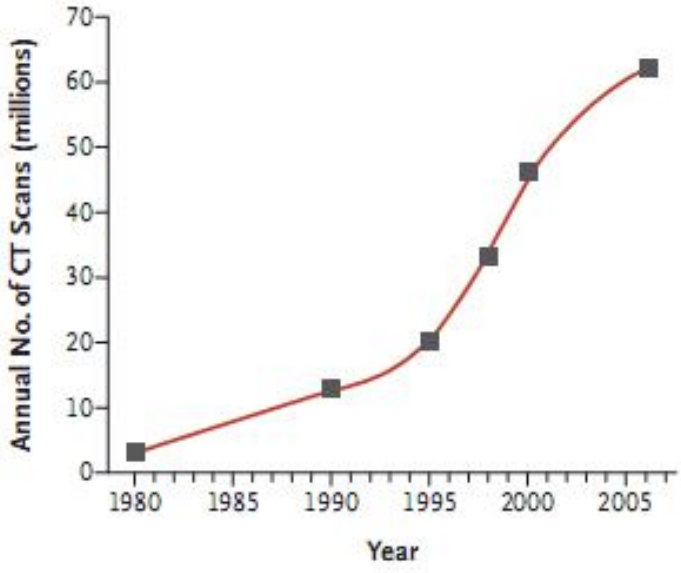


Fig. 2.3.3 **Estimated Number of CT Scans Performed Annually in the United States.**

The most recent estimate of 62 million CT scans in 2006 is from an IMV CT Market Summary Report.[3]

www.najm.org

## 2.4 Brain anatomy:

### 2.4.1 Nervous system:

The nervous system is divided into central and peripheral systems. The central nervous system (CNS) is composed of the brain and spinal cord. The peripheral nervous system (PNS) is composed of spinal nerves that branch from the spinal cord and cranial nerves that branch from the brain. The PNS includes the autonomic nervous system, which controls vital functions such as breathing, digestion, heart rate, and secretion of hormones **(www.mayfieldclinic.com)**.

### 2.4.2 Skull:

The purpose of the bony skull is to protect the brain from injury. The skull is formed from 8 bones that fuse together along suture lines. These bones include the frontal, parietal (2), temporal (2), sphenoid, occipital and ethmoid (Fig 2.4.1). The face is formed from 14 paired bones including the maxilla , zygoma, nasal, palatine, lacrimal, inferior nasal conchae, mandible, and vomer **(www.mayfieldclinic.com)**..

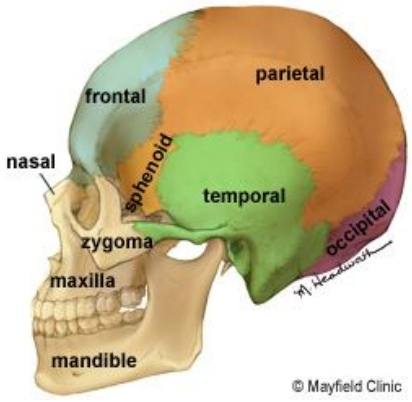


**Figure 2.4.1 Eight bones form the skull and fourteen bones form the face. (www.mayfieldclinic.com)**

Inside the skull are three distinct areas: anterior fossa, middle fossa, and posterior fossa (Fig. 2.4.2). Doctors sometimes refer to a tumor's location by these terms, e.g., middle fossa meningioma **(www.mayfieldclinic.com)**..

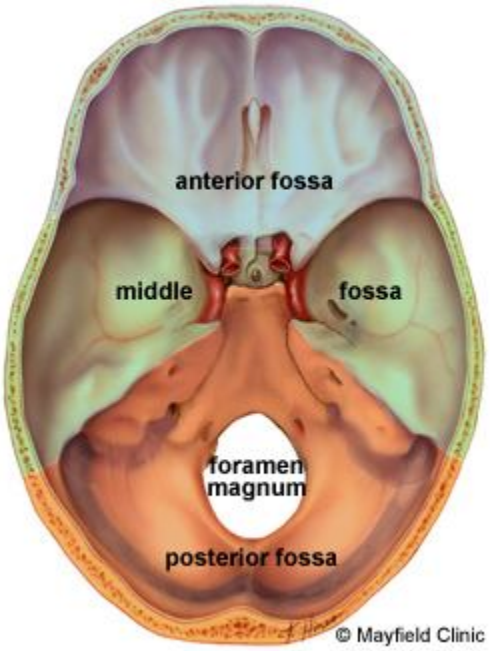


**Figure 2.4.2 The inside of the skull is divided into three areas called the anterior, middle, and posterior fossae.(www.mayfieldclinic.com)**

Similar to cables coming out the back of a computer, all the arteries, veins and nerves exit the base of the skull through holes, called foramina. The big hole in the middle (foramen magnum) is where the spinal cord exits **(www.mayfieldclinic.com)**..

### 2.4.3Brain

The brain is composed of the cerebrum, cerebellum, and brainstem (Fig. 2.4.3).

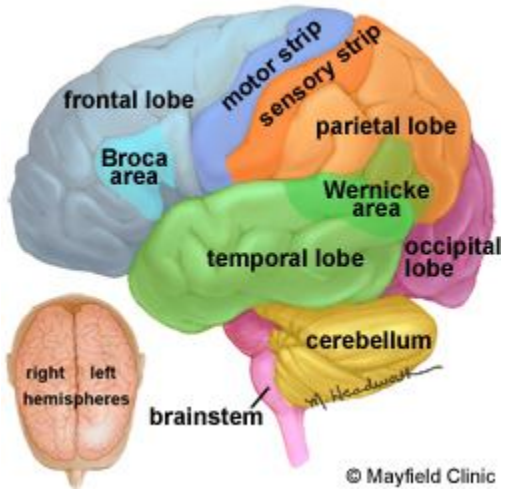


**Figure2.4.3 The brain is composed of three parts: the brainstem, cerebellum, and cerebrum.**
**The cerebrum is divided into four lobes: frontal, parietal, temporal, and occipital (www.mayfieldclinic.com)**.

The **cerebrum** is the largest part of the brain and is composed of right and left hemispheres. It performs higher functions like interpreting touch, vision and hearing, as well as speech, reasoning, emotions, learning, and fine control of movement **(www.mayfieldclinic.com)**..

The **cerebellum** is located under the cerebrum. Its function is to coordinate muscle movements, maintain posture, and balance **(www.mayfieldclinic.com)**..

The **brainstem** includes the midbrain, pons, and medulla. It acts as a relay center connecting the cerebrum and cerebellum to the spinal cord. It performs many automatic functions such as breathing, heart rate, body temperature, wake and sleep cycles, digestion, sneezing, coughing, vomiting, and swallowing. Ten of the twelve cranial nerves originate in the brainstem **(www.mayfieldclinic.com)**.

The surface of the cerebrum has a folded appearance called the cortex. The cortex contains about 70% of the 100 billion nerve cells. The nerve cell bodies color the cortex grey-brown giving it its name – gray matter (Fig. 2.4.4). Beneath the cortex are long connecting fibers between neurons, called axons, which make up the white matter **(www.mayfieldclinic.com)**.


**Figure 2.4.4 The surface of the cerebrum is called the cortex. The cortex contains neurons (grey matter), which are interconnected to other brain areas by axons (white matter). The cortex has a folded appearance. A fold is called a gyrus and the groove between is a sulcus (www.mayfieldclinic.com)**.

The folding of the cortex increases the brain's surface area allowing more neurons to fit inside the skull and enabling higher functions. Each fold is called a gyrus, and each groove between folds is called a sulcus. There are

names for the folds and grooves that help define specific brain regions **(www.mayfieldclinic.com)**.

### 2.4.4 Right brain – left brain:

The right and left hemispheres of the brain are joined by a bundle of fibers called the corpus callosum that delivers messages from one side to the other. Each hemisphere controls the opposite side of the body. If a brain tumor is located on the right side of the brain, your left arm or leg may be weak or paralyzed **(www.mayfieldclinic.com)**.

Not all functions of the hemispheres are shared. In general, the left hemisphere controls speech, comprehension, arithmetic, and writing. The right hemisphere controls creativity, spatial ability, artistic, and musical skills. The left hemisphere is dominant in hand use and language in about 92% of people**(www.mayfieldclinic.com)**.

### 2.4.5 Lobes of the brain:

The cerebral hemispheres have distinct fissures, which divide the brain into lobes. Each hemisphere has 4 lobes: frontal, temporal, parietal, and occipital (Fig 2.4.3). Each lobe may be divided, once again, into areas that serve very specific functions. It's important to understand that each lobe of the brain does not function alone. There are very complex relationships between the lobes of the brain and between the right and left hemispheres **(www.mayfieldclinic.com)**.

### 2.4.6 Frontal lobe

Personality, behavior, emotions .

Judgment, planning, problem solving .

Speech: speaking and writing (Broca's area).

Body movement (motor strip) .

Intelligence, concentration, self awareness.

**2.4.7 Parietal lobe:**

Interprets language, words .

Sense of touch, pain, temperature (sensory strip) .

Interprets signals from vision, hearing, motor, sensory and memory.

Spatial and visual perception .

**2.4.8 Occipital lobe:**

Interprets vision (color, light, movement).

## 2.4.9 Temporal lobe:

Understanding language (Wernicke's area).

Memory.

Hearing.

Sequencing and organization.

Messages within the brain are carried along pathways. Messages can travel from one gyrus to another, from one lobe to another, from one side of the brain to the other, and to structures found deep in the brain (e.g. thalamus, hypothalamus) **(www.mayfieldclinic.com)**.

**2.4.10 Deep structures:**

**2..4.10.1 Hypothalamus -** is located in the floor of the third ventricle and is the master control of the autonomic system. It plays a role in controlling behaviors such as hunger, thirst, sleep, and sexual response. It also regulates body temperature, blood pressure, emotions, and secretion of hormones **(www.mayfieldclinic.com)**.

**2.4.10.2 Pituitary gland** - lies in a small pocket of bone at the skull base called the sella turcica. The pituitary gland is connected to the hypothalamus of the brain by the pituitary stalk. Known as the "master gland," it controls other endocrine glands in the body. It secretes hormones that control sexual development, promote bone and muscle growth, respond to stress, and fight disease **(www.mayfieldclinic.com)**.

**2.4.10.3 Pineal gland** - is located behind the third ventricle. It helps regulate the body's internal clock and circadian rhythms by secreting melatonin. It has some role in sexual development **(www.mayfieldclinic.com)**.

**2.4.10.4 Thalamus** - serves as a relay station for almost all information that comes and goes to the cortex (Fig. 2.4.5). It plays a role in pain sensation, attention, alertness and memory **(www.mayfieldclinic.com)**.

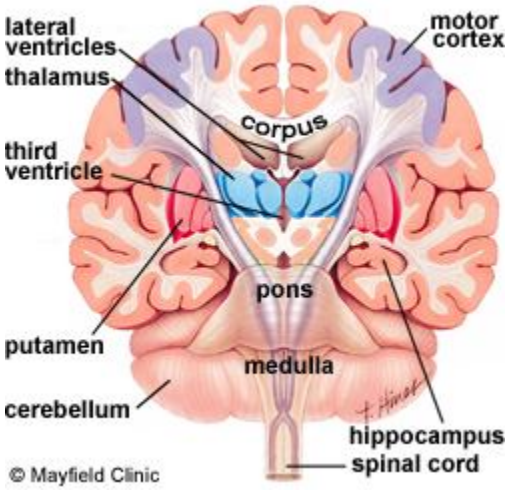


**Figure 2.4.5 Coronal cross-section showing the basal ganglia (www.mayfieldclinic.com)**.

**2.4.10.5 Basal ganglia** - includes the caudate, putamen and globus pallidus. These nuclei work with the cerebellum to coordinate fine motions, such as fingertip movements**(www.mayfieldclinic.com)**.

**2.4.10.6 Limbic system** - is the center of our emotions, learning, and memory. Included in this system are the cingulate gyri, hypothalamus, amygdala (emotional reactions) and hippocampus (memory) **(www.mayfieldclinic.com)**.

**2.4.10.5 Cranial nerves:**

The brain communicates with the body through the spinal cord and twelve pairs of cranial nerves (Fig. 2.4.6). Ten of the twelve pairs of cranial nerves that control hearing, eye movement, facial sensations, taste, swallowing and movement of the face, neck, shoulder and tongue muscles originate in the brainstem. The cranial nerves for smell and vision originate in the cerebrum**(www.mayfieldclinic.com)**.

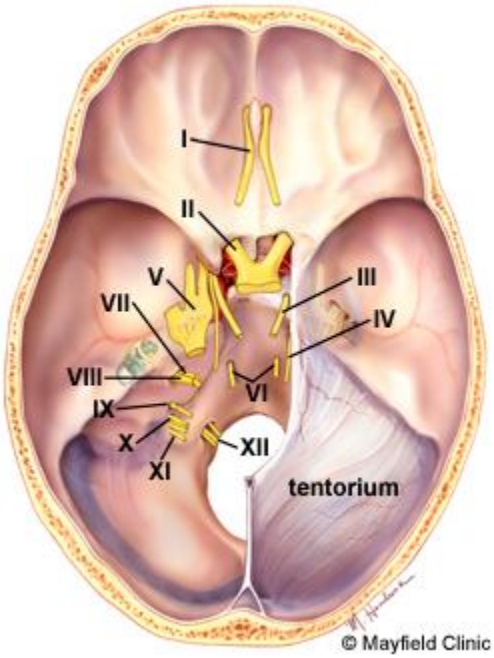


**Figure 2.4.6 The Roman numeral, name, and main function of the twelve cranial nerves (www.mayfieldclinic.com)**.

| **Number** | **Name** | **Function** |
|---|---|---|
| I | Olfactory | Smell |
| II | Optic | Sight |
| III | Oculomotor | moves eye, pupil |
| IV | Trochlear | moves eye |
| V | Trigeminal | face sensation |
| VI | Abducens | moves eye |
| VII | Facial | moves face, salivate |
| VIII | vestibulocochlear | hearing, balance |
| IX | glossopharyngeal | taste, swallow |

| | | |
|---|---|---|
| X | Vagus | heart rate, digestion |
| XI | Accessory | moves head |
| XII | Hypoglossal | moves tongue |

**Table 2.4.1 sensations and function (www.mayfieldclinic.com)**.

### 2.4.11 Meninges:

The brain and spinal cord are covered and protected by three layers of tissue called meninges. From the outermost layer inward they are: the dura mater, arachnoid mater, and pia mater**(www.mayfieldclinic.com)**.

The dura mater is a strong, thick membrane that closely lines the inside of the skull; its two layers, the periosteal and meningeal dura, are fused and separate only to form venous sinuses. The dura creates little folds or compartments. There are two special dural folds, the falx and the tentorium. The falx separates the right and left hemispheres of the brain and the tentorium separates the cerebrum from the cerebellum **(www.mayfieldclinic.com)**.

The arachnoid mater is a thin, web-like membrane that covers the entire brain. The arachnoid is made of elastic tissue. The space between the dura and arachnoid membranes is called the subdural space **(www.mayfieldclinic.com)**.

The pia mater hugs the surface of the brain following its folds and grooves. The pia mater has many blood vessels that reach deep into the brain. The space between the arachnoid and pia is called the subarachnoid space. It is

here where the cerebrospinal fluid bathes and cushions the brain **(www.mayfieldclinic.com)**.

### 2.4.12 Ventricles and cerebrospinal fluid:

The brain has hollow fluid-filled cavities called ventricles (Fig. 2.4.7). Inside the ventricles is a ribbon-like structure called the choroid plexus that makes clear colorless cerebrospinal fluid (CSF). CSF flows within and around the brain and spinal cord to help cushion it from injury. This circulating fluid is constantly being absorbed and replenished **(www.mayfieldclinic.com)**.

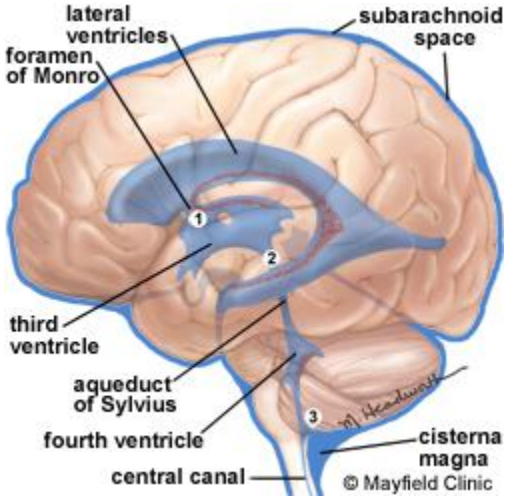


**Figure 2.4.7 CSF is produced inside the ventricles deep within the brain. CSF fluid circulates inside the brain and spinal cord and then outside to the subarachnoid space. Common sites of obstruction: 1) foramen of Monro, 2) aqueduct of Sylvius, and 3) obex (www.mayfieldclinic.com)**.

There are two ventricles deep within the cerebral hemispheres called the lateral ventricles. They both connect with the third ventricle through a separate opening called the foramen of Monro. The third ventricle connects with the fourth ventricle through a long narrow tube called the aqueduct of

Sylvius. From the fourth ventricle, CSF flows into the subarachnoid space where it bathes and cushions the brain. CSF is recycled (or absorbed) by special structures in the superior sagittal sinus called arachnoid villi **(www.mayfieldclinic.com)**.

A balance is maintained between the amount of CSF that is absorbed and the amount that is produced. A disruption or blockage in the system can cause a build up of CSF, which can cause enlargement of the ventricles (hydrocephalus) or cause a collection of fluid in the spinal cord (syringomyelia) **(www.mayfieldclinic.com)**.

### 2.4.13 Blood supply:

Blood is carried to the brain by two paired arteries, the internal carotid arteries and the vertebral arteries (Fig. 8). The internal carotid arteries supply most of the cerebrum **(www.mayfieldclinic.com)**.

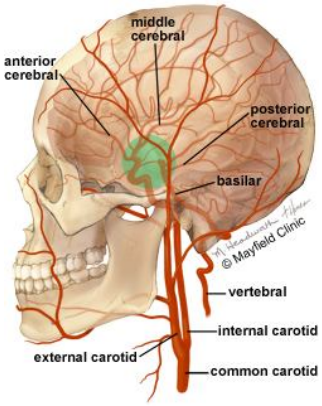


**Figure2.4.8 The common carotid artery courses up the neck and divides into the internal and external carotid arteries. The brain's anterior circulation is fed by the internal carotid arteries (ICA) and the posterior circulation is fed by the vertebral arteries (VA). The two systems connect at the Circle of Willis (green circle) (www.mayfieldclinic.com)**.

The vertebral arteries supply the cerebellum, brainstem, and the underside of the cerebrum. After passing through the skull, the right and left vertebral arteries join together to form the basilar artery. The basilar artery and the internal carotid arteries "communicate" with each other at the base of the brain called the Circle of Willis (Fig. 2.4.9). The communication between the internal carotid and vertebral-basilar systems is an important safety feature of the brain. If one of the major vessels becomes blocked, it is possible for collateral blood flow to come across the Circle of Willis and prevent brain damage **(www.mayfieldclinic.com)**.

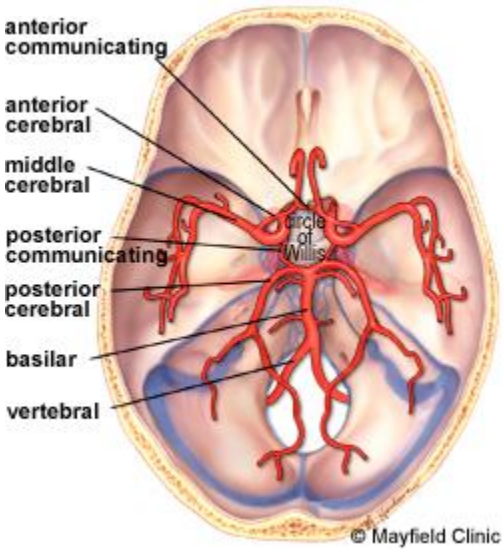


**Figure 2.4.9 Top view of the Circle of Willis. The internal carotid and vertebral-basilar systems are joined by the anterior communicating and posterior communicating arteries (www.mayfieldclinic.com)**.

The venous circulation of the brain is very different than the rest of the body. Usually arteries and veins run together as they supply and drain specific areas of the body. So one would think there would be a pair of vertebral veins and internal carotid veins. However, this is not the case in the brain.

The major vein collectors are integrated into the dura to form venous sinuses (Fig. 2.4.10) - not to be confused with the air sinuses in the face and nasal region. The venous sinuses collect the blood from the brain and pass it to the internal jugular veins. The superior and inferior sagittal sinuses drain the cerebrum, the cavernous sinuses drains the anterior skull base. All sinuses eventually drain to the sigmoid sinuses, which exit the skull and form the jugular veins. These two jugular veins are essentially the only drainage of the brain **(www.mayfieldclinic.com)**.

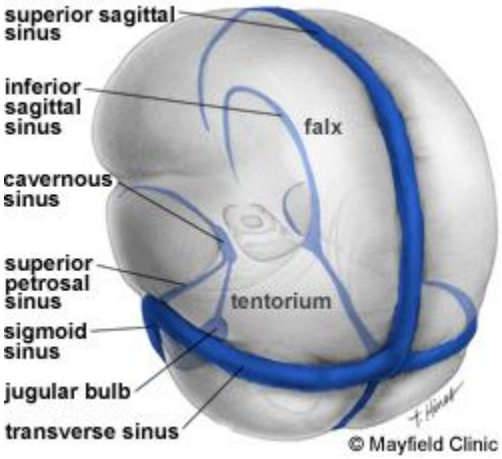


**Figure 2.4.10 three quarter view of the dural covering of the brain depicts the two major dural folds, the falx and tentorium along with the venous sinuses (www.mayfieldclinic.com)**.

### 2.4.14 Language:

In general, the left hemisphere of the brain is responsible for language and speech and is called the "dominant" hemisphere. The right hemisphere plays a large part in interpreting visual information and spatial processing. In about one third of individuals who are left-handed, speech function may be located on the right side of the brain. Left-handed individuals may need

special testing to determine if their speech center is on the left or right side prior to any surgery in that area **(www.mayfieldclinic.com)**.

Aphasia is a disturbance of language affecting production, comprehension, reading or writing, due to brain injury – most commonly from stroke or trauma. The type of aphasia depends on the brain area affected **(www.mayfieldclinic.com)**.

**2.4.14.1 Broca's area** lies in the left frontal lobe (Fig 2.4.3). If this area is damaged, one may have difficulty moving the tongue or facial muscles to produce the sounds of speech. The individual can still read and understand spoken language but has difficulty in speaking and writing (i.e. forming letters and words, doesn't write within lines) – called Broca's aphasia **(www.mayfieldclinic.com)**.

**2.4.14.2 Wernicke's area** lies in the left temporal lobe (Fig 2.4.3). Damage to this area causes Wernicke's aphasia. The individual may speak in long sentences that have no meaning, add unnecessary words, and even create new words. They can make speech sounds, however they have difficulty understanding speech and are therefore unaware of their mistakes **(www.mayfieldclinic.com)**.

**2.4.15 Memory:**

Memory is a complex process that includes three phases: encoding (deciding what information is important), storing, and recalling. Different areas of the brain are involved in memory depending on the type of memory **(www.mayfieldclinic.com)**.

**2.4.15.1 Short-term memory**, also called working memory, occurs in the prefrontal cortex. It stores information for about one minute and its capacity is limited to about 7 items. For example, it enables you to dial a phone number someone just told you. It also intervenes during reading, to memorize the sentence you have just read, so that the next one makes sense **(www.mayfieldclinic.com)**.

**2.4.15.2 Long-term memory** is processed in the hippocampus of the temporal lobe and is activated when you want to memorize something for a longer time. This memory has unlimited content and duration capacity. It contains personal memories as well as facts and figures **(www.mayfieldclinic.com)**.

**2.4.15.3 Skill memory** is processed in the cerebellum, which relays information to the basal ganglia. It stores automatic learned memories like tying a shoe, playing an instrument, or riding a bike **(www.mayfieldclinic.com)**.

### 2.4.16 Cells of the brain

The brain is made up of two types of cells: nerve cells (neurons) and glia cells **(www.mayfieldclinic.com)**.

### 2.4.16.1Nerve cells

There are many sizes and shapes of neurons, but all consist of a cell body, dendrites and an axon. The neuron conveys information through electrical and chemical signals. Try to picture electrical wiring in your home. An electrical circuit is made up of numerous wires connected in such a way that

when a light switch is turned on, a light bulb will beam. A neuron that is excited will transmit its energy to neurons within its vicinity **(www.mayfieldclinic.com)**.

Neurons transmit their energy, or "talk", to each other across a tiny gap called a synapse (Fig. 2.4.11). A neuron has many arms called dendrites, which act like antennae picking up messages from other nerve cells. These messages are passed to the cell body, which determines if the message should be passed along. Important messages are passed to the end of the axon where sacs containing neurotransmitters open into the synapse. The neurotransmitter molecules cross the synapse and fit into special receptors on the receiving nerve cell, which stimulates that cell to pass on the message **(www.mayfieldclinic.com)**.

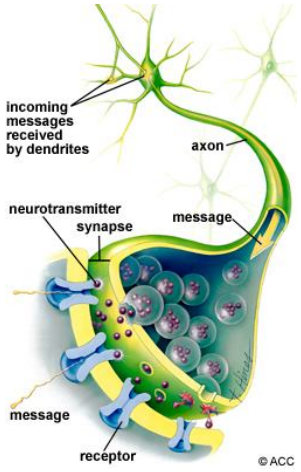


**Figure2.4.11.Nerve cells consist of a cell body, dendrites and axon. Neurons communicate with each other by exchanging neurotransmitters across a tiny gap called a synapse (www.mayfieldclinic.com)**.

### 2.4.16.2 Glia cells:

Glia (Greek word meaning glue) is the cells of the brain that provide neurons with nourishment, protection, and structural support. There are about 10 to 50 times more glia than nerve cells and are the most common type of cells involved in brain tumors **(www.mayfieldclinic.com)**.

Astroglia or astrocytes transport nutrients to neurons, hold neurons in place, digest parts of dead neurons, and regulate the blood brain barrier.

Oligodendroglia cells provide insulation (myelin) to neurons **(www.mayfieldclinic.com)**.

Ependymal cells line the ventricles and secrete cerebrospinal fluid (CSF).

Microglia digest dead neurons and pathogens (www.mayfield clinic.com) **.**

## 2.5 CT brain protocols:

### 2.5.1 CT Scan of the Head:

Computed tomography, more commonly known as a CT or CAT scan, is a diagnostic medical test that, like traditional x-rays, produces multiple images or pictures of the inside of the body(*www.RadiologyInfo.org).*

The cross-sectional images generated during a CT scan can be reformatted in multiple planes, and can even generate three-dimensional images. These images can be viewed on a computer monitor, printed on film or transferred to a CD or DVD(*www.RadiologyInfo.org).*.

CT images of internal organs, bones, soft tissue and blood vessels typically provide greater detail than traditional x-rays, particularly of soft tissues and blood vessels. (*www.RadiologyInfo.org).*

CT scanning provides more detailed information on head injuries, stroke, brain tumors and other brain diseases than regular radiographs (x-rays) (*www.RadiologyInfo.org).*.

### 2.5.2 common uses of the procedure:

#### 2.5.2.1 CT scanning of the head is typically used to detect:

bleeding, brain injury and skull fractures in patients with head injuries.

bleeding caused by a ruptured or leaking aneurysm in a patient with a sudden severe headache(*www.RadiologyInfo.org).*.

a blood clot or bleeding within the brain shortly after a patient exhibits symptoms of a stroke.

a stroke, especially with a new technique called Perfusion CT.

brain tumors.

enlarged brain cavities (ventricles) in patients with hydrocephalus.

diseases or malformations of the skull. (*www.RadiologyInfo.org)*.

**2.5.2.2 CT scanning is also performed to:**

evaluate the extent of bone and soft tissue damage in patients with facial trauma, and planning surgical reconstruction.

diagnose diseases of the temporal bone on the side of the skull, which may be causing hearing problems.

determine whether inflammation or other changes are present in the paranasal sinuses.

plan radiation_therapy for cancer of the brain or other tissues.

guide the passage of a needle used to obtain a tissue sample (biopsy) from the brain.

assess aneurysms or arteriovenous malformations through a technique called CT angiography. (*www.RadiologyInfo.org)*.

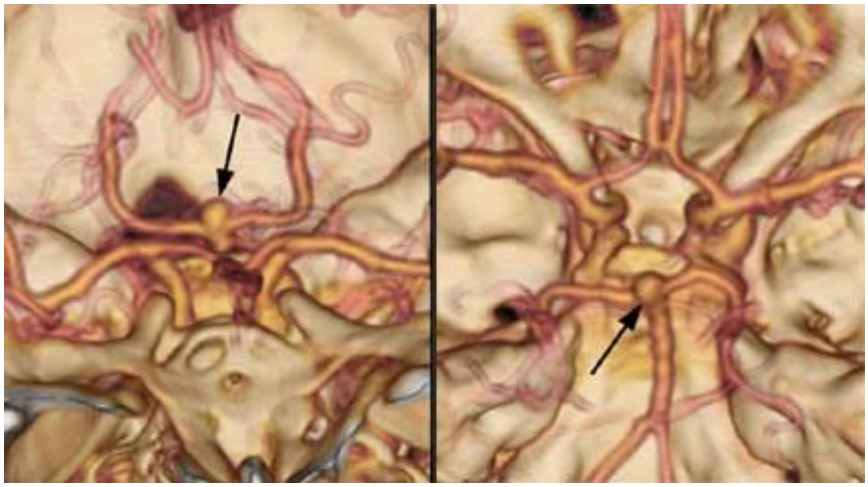

Figure 2.5.1 CT angiography (*www.RadiologyInfo.org).*

**2.5.3 Preparation:**

You should wear comfortable, loose-fitting clothing to your exam. You may be given a gown to wear during the procedure.

Metal objects, including jewelry, eyeglasses, dentures and hairpins, may affect the CT images and should be left at home or removed prior to your exam. You may also be asked to remove hearing aids and removable dental work. Women will be asked to remove bras containing metal underwire. You may be asked to remove any piercings, if possible(*www.RadiologyInfo.org).*.

You should inform the technologist if you have a pacemaker. Pacemakers do not hinder the use of CT as in MRI as long as the scanner will not be taking images repeatedly over the area of the pacemaker device in the upper chest. This is usually not an issue for cardiac CT exams(*www.RadiologyInfo.org).*.

You may be asked not to eat or drink anything for a few hours beforehand, especially if a contrast material will be used in your exam. You should inform your physician of all medications you are taking and if you have any allergies. If you have a known allergy to contrast material, or "dye," your doctor may prescribe medications (usually a steroid) to reduce the risk of an allergic reaction. These medications generally need to be taken 12 hours prior to administration of contrast material. To avoid unnecessary delays, contact your doctor before the exact time of your exam(*www.RadiologyInfo.org)*..

Also inform your doctor of any recent illnesses or other medical conditions and whether you have a history of heart disease, asthma, diabetes, kidney disease or thyroid problems. Any of these conditions may increase the risk of an unusual adverse effect.

The radiologist also should know if you have asthma, multiple_myeloma or any disorder of the heart, kidneys or thyroid_gland, or if you have diabetes particularly if you are taking Glucophage.

Women should always inform their physician and the CT technologist if there is any possibility that they may be pregnant(*www.RadiologyInfo.org)*..

### 2.5.4 The equipment:

**Figure 2.5.2 CT imaging device** (*www.RadiologyInfo.org).*

The CT scanner is typically a large, box-like machine with a hole, or short tunnel, in the center. You will lie on a narrow examination table that slides into and out of this tunnel. Rotating around you, the x-ray tube and electronic x-ray detectors are located opposite each other in a ring, called a gantry. The computer workstation that processes the imaging information is located in a separate control room, where the technologist operates the scanner and monitors your examination in direct visual contact and usually with the ability to hear and talk to you with the use of a speaker and microphone(*www.RadiologyInfo.org).*.

**2.5.5 procedure work:**

**Figure 2.5.3 CT for brain** (*www.RadiologyInfo.org).*

In many ways CT scanning works very much like other x-ray examinations. Different body parts absorb the x-rays in varying degrees. It is this crucial difference in absorption that allows the body parts to be distinguished from one another on an x-ray film or CT electronic image(*www.RadiologyInfo.org).*.

In a conventional x-ray exam, a small amount of radiation is aimed at and passes through the part of the body being examined, recording an image on a special electronic image recording plate. Bones appear white on the x-ray; soft tissue, such as organs like the heart or liver, shows up in shades of gray, and air appears black(*www.RadiologyInfo.org).*.

With CT scanning, numerous x-ray beams and a set of electronic x-ray detectors rotate around you, measuring the amount of radiation being absorbed throughout your body. Sometimes, the examination table will move during the scan, so that the x-ray beam follows a spiral path. A special computer program processes this large volume of data to create two-dimensional cross-sectional images of your body, which are then displayed on a monitor. CT imaging is sometimes compared to looking into a loaf of bread by cutting the loaf into thin slices. When the image slices are reassembled by computer software, the result is a very detailed multidimensional view of the body's interior (*www.RadiologyInfo.org)*..

Refinements in detector technology allow new CT scanners to obtain multiple slices in a single rotation. These scanners, called multislice CT or multidetector CT, allow thinner slices to be obtained in a shorter period of time, resulting in more detail and additional view capabilities.

Modern CT scanners are so fast that they can scan through large sections of the body in just a few seconds, and even faster in small children. Such speed is beneficial for all patients but especially children, the elderly and critically ill, all of whom may have difficulty in remaining still, even for the brief time necessary to obtain images.

For children, the CT scanner technique will be adjusted to their size and the area of interest to reduce the radiation dose.

For some CT exams, a contrast material is used to enhance visibility in the area of the body being studied(*www.RadiologyInfo.org)*..

**2.5.6 Procedure performance:**

The technologist begins by positioning you on the CT examination table, usually lying flat on your back or less commonly, on your side or on your stomach. Straps and pillows may be used to help you maintain the correct position and to help you remain still during the exam. Depending on the part of the body being scanned, you may be asked to raise your arms over your head(*www.RadiologyInfo.org)*..

Many scanners are fast enough that children can be scanned without sedation. In special cases, sedation may be needed for children who cannot hold still. Motion will degrade the quality of the examination the same way that it affects photographs(*www.RadiologyInfo.org)*..

If contrast material is used, depending on the type of exam, it will be swallowed, injected through an intravenous line (IV) or administered by enema (this is rare) (*www.RadiologyInfo.org)*..

Next, the table will move quickly through the scanner to determine the correct starting position for the scans. Then, the table will move slowly through the machine as the actual CT scanning is performed. Depending on the type of CT scan, the machine may make several passes(*www.RadiologyInfo.org)*..

You may be asked to hold your breath during the scanning. Any motion, whether breathing or body movements, can lead to artifacts on the images. This loss of image quality can resemble the blurring seen on a photograph taken of a moving object(*www.RadiologyInfo.org)*..

When the examination is completed, you will be asked to wait until the technologist verifies that the images are of high enough quality for accurate interpretation(*www.RadiologyInfo.org)*..

A CT scan of the head is usually completed within 10 minutes(*www.RadiologyInfo.org)*..

### 2.5.7 Experience during and after the procedure:

CT exams are generally painless, fast and easy. With multidetector CT, the amount of time that the patient needs to lie still is reduced.

Though the scanning itself causes no pain, there may be some discomfort from having to remain still for several minutes. If you have a hard time staying still, are claustrophobic or have chronic pain, you may find a CT exam to be stressful. The technologist or nurse, under the direction of a physician, may offer you some medication to help you tolerate the CT scanning procedure(*www.RadiologyInfo.org)*..

If an intravenous contrast material is used, you will feel a pin prick when the needle is inserted into your vein. You will likely have a warm, flushed sensation during the injection of the contrast materials and a metallic taste in your mouth that lasts for at most a minute or two. You may experience a sensation like you have to urinate; however, this is actually a contrast effect and subsides quickly(*www.RadiologyInfo.org)*..

When you enter the CT scanner room, special light lines may be seen projected onto your body, and are used to ensure that you are properly positioned. With modern CT scanners, you will hear only slight buzzing,

clicking and whirring sounds as the CT scanner revolves around you during the imaging process(*www.RadiologyInfo.org)*..

You will be alone in the exam room during the CT scan, unless there are special circumstances. For example, sometimes a parent wearing a lead shield may stay in the room with their child. However, the technologist will always be able to see, hear and speak with you through a built-in intercom system(*www.RadiologyInfo.org)*..

With pediatric patients, a parent may be allowed in the room but will be required to wear a lead apron to minimize radiation exposure.

After a CT exam, you can return to your normal activities. If you received contrast material, you may be given special instructions(*www.RadiologyInfo.org)*..

**2.5.8 Interpretation of the results:**

A physician, usually a radiologist with expertise in supervising and interpreting radiology examinations, will analyze the images and send a signed report to your primary care physician or physician who referred you for the exam, who will discuss the results with you(*www.RadiologyInfo.org)*..

Follow-up examinations may be necessary, and your doctor will explain the exact reason why another exam is requested. Sometimes a follow-up exam is done because a suspicious or questionable finding needs clarification with additional views or a special imaging technique. A follow-up examination may also be necessary so that any change in a known abnormality can be

monitored over time. Follow-up examinations are sometimes the best way to see if treatment is working or if an abnormality is stable over time(*www.RadiologyInfo.org)*..

## 2.6 Previous study:

In the study by mathin etal conventional mode, the highest surface dose was 83.2 mGy (scanner 1:helical mode, 55.6 mGy), and 66.0 mGy (scanner 2: helical mode, 55.9 mGy). By changing kVp and mAs, a dose reduction of up to 75% (scanner 1), and 60% (scanner 2) was achieved. No observable differences in image quality between scans obtained with doses from 100% to 60% of standard settings were noted. Ten of 20 images obtained with the highest dose and 13 of 20 images obtained with lowest dose (19–29.4 mGy) were reliably identified by subjective quality assessment. Scans produced with a surface dose of less than 30 mGy were judged uninterpretable.

### 2.6.1 CONCLUSION:

Standard parameters used in cranial CT are oriented toward best image quality. A dose reduction up to 40% may be possible without loss of diagnostic image quality.

# Chapter three

## Material and method

### 3.1 Material:

### 3.1.1 Patients:

30 patients with average age 6month to70 years all of them under went CT study for brain with different protocols, CTDI and DLP were obtained.

### 3.1.2 Machine used:

| Machine unit | Maximum mAS | Maximum kv | Year of installation | Type of acquisition | Manufacturer |
|---|---|---|---|---|---|
| CT/dual | 624 | 140 | 2003 | Indirect acquisition | American |
| CT 64 slices | 500 | 140 | 2010 | Direct acquisition | Japanese |
| CT 16 slices | 624 | 140 | 2010 | Indirect acquisition | Chinese |

**Table 3.1**

### 3.2Method:

### 3.2.1 Technique used:

Patient lie on the scan table, the head immobilized to prevent movement during the procedure. A localizer radiograph is taken prior to the actual CT procedure, axial scan started from the base of the skull to vertex. Patient

suspected to have tumors will undergo similar axial scan with an intravenous (IV).

### 3.2.2 Data interpretation:

In this thesis information taken from patients who underwent CT brain study, the data taken for 30 patients for posterior fossa and supra sella region each for(kv, mAs, CTDI, DLP, scan time, slice thickness and number of slices) we focus on radiation dose (DLP) and how it influences by mAs , scan time , slice thickness and number of slices. Also we compare between DLP and image quality(SNR and spatial resolution), SNR and spatial resolution evaluated subjectively by four radiologist whom they relatively visualize the picture and classified it in to five grades(excellent, v.good, good, acceptable and poor) . Also a comparison made between artifacts and scan time.

# Chapter four

## Results:

## 4.1 general characteristics of the sample studied:

## Table4.1 gender distribution:

| Sex | Frequency | percentage |
|---|---|---|
| Male | 13 | 43.3% |
| Female | 17 | 56.7% |
| Total | 30 | 100% |

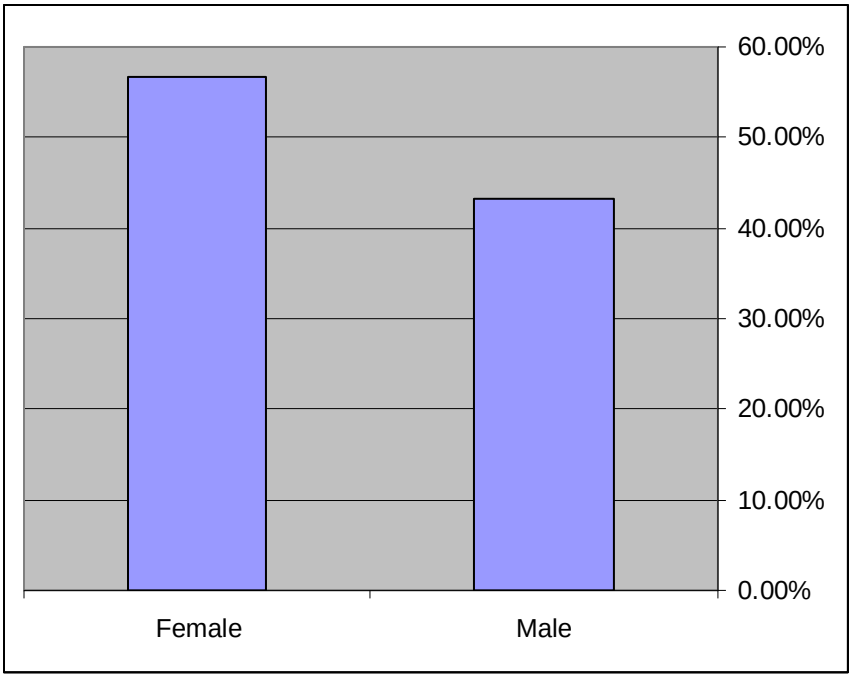


## Figure 4.1 gender distribution:

## Table 4.2 age distribution:

| Age | Frequency | percentage |
|---|---|---|
| <1 year | 2 | 6.7% |
| 1-<5 years | 2 | 2.7% |
| 5-<10 years | 1 | 3.3% |
| 10-<20 years | 9 | 30% |
| 20-<30 years | 4 | 13.3% |
| 30-70 years | 12 | 40% |
| Total | 30 | 100% |

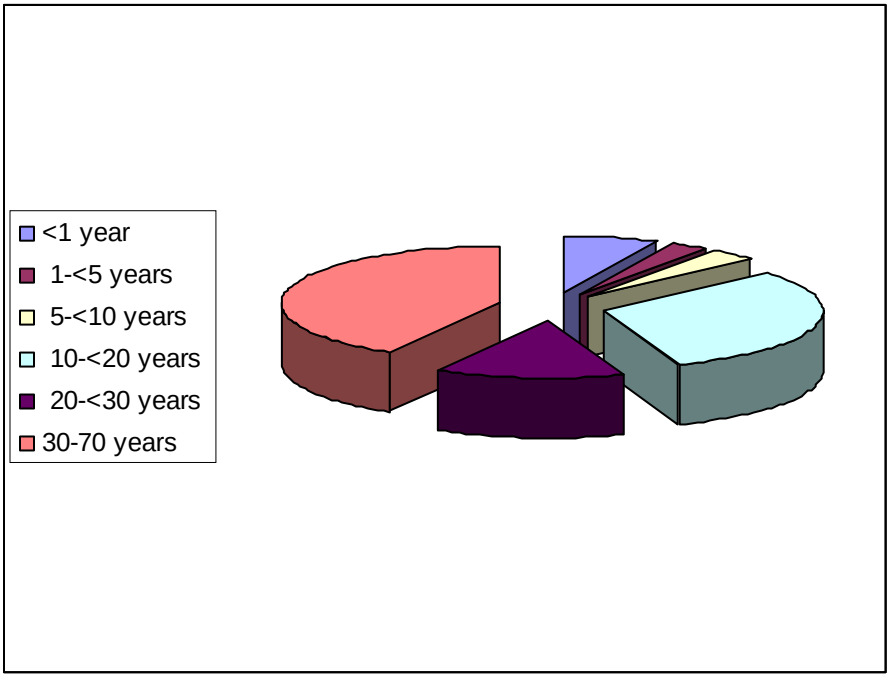


## Figure 4.2 age distribution:

## 4.2 cross tabulation:

We gathered the following results from three centers in Khartoum state. It shows CT brain imaging parameters and CT image quality:

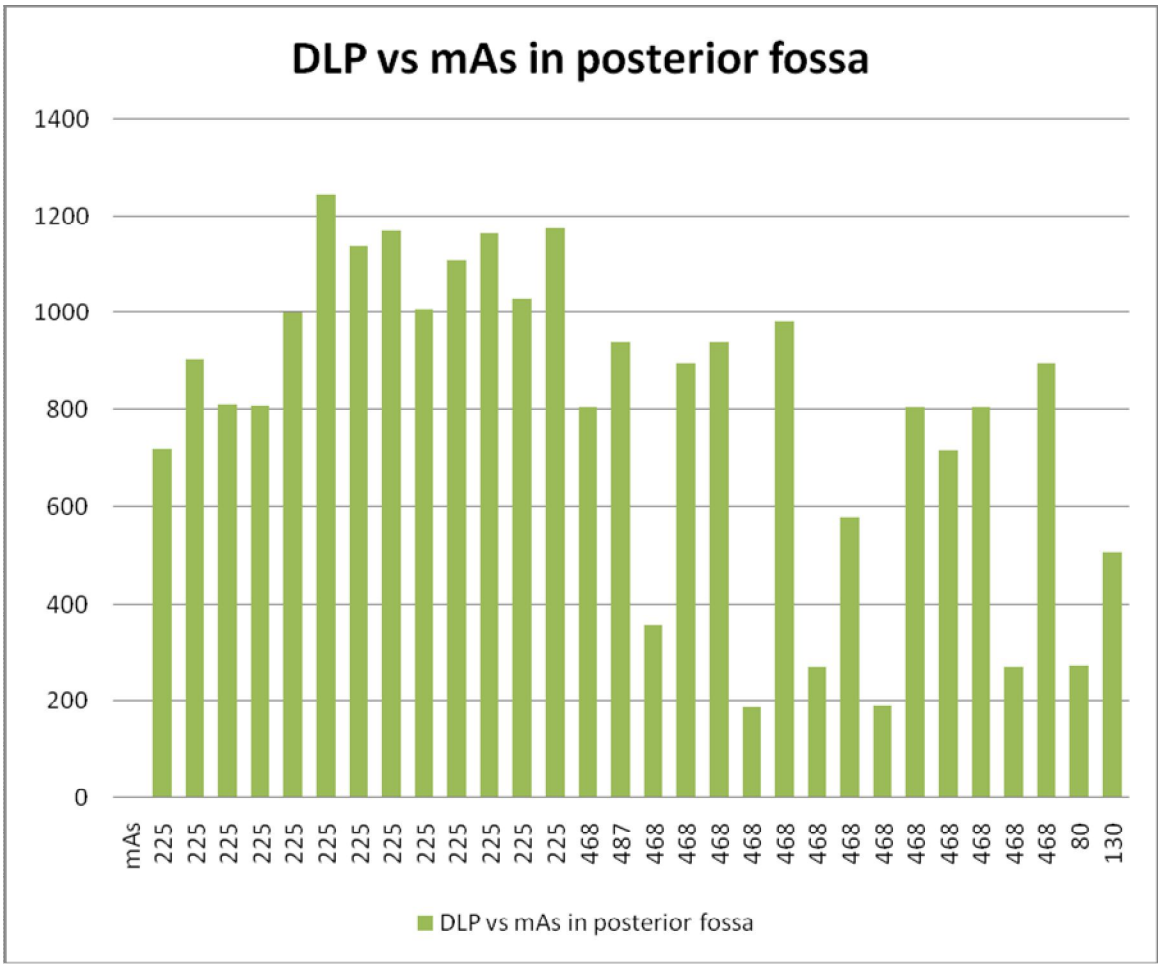


**Figure 4.3 DLP vs  mAs in posterior fossa**

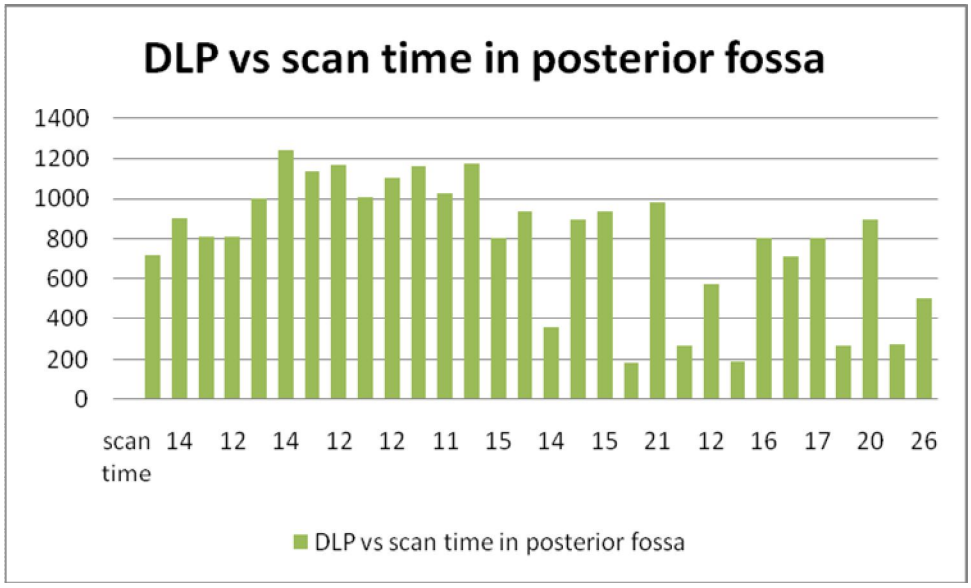


**Figure 4.4 DLP vs scan time in posterior fossa**

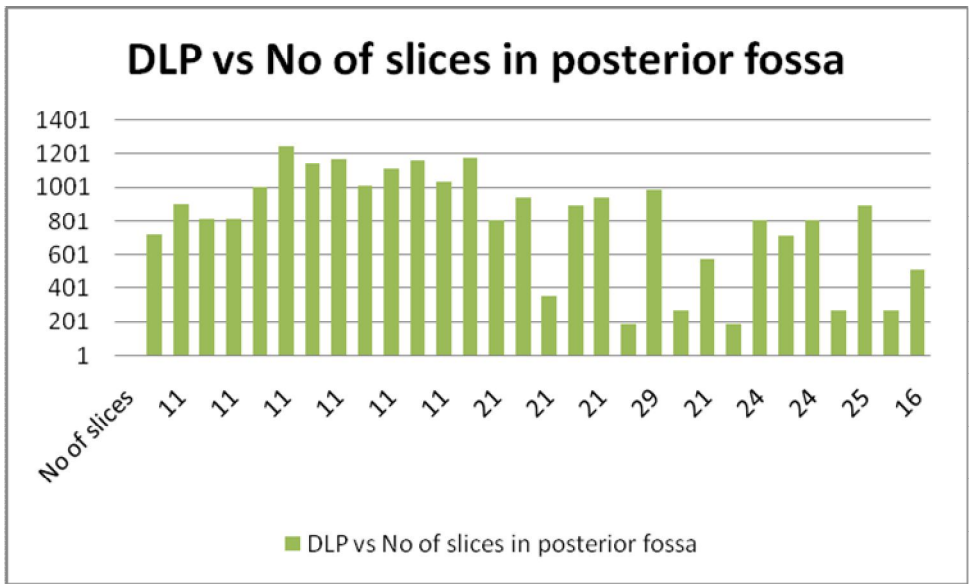


**Figure 4.5 DLP vs NO. of slices in posterior fossa**

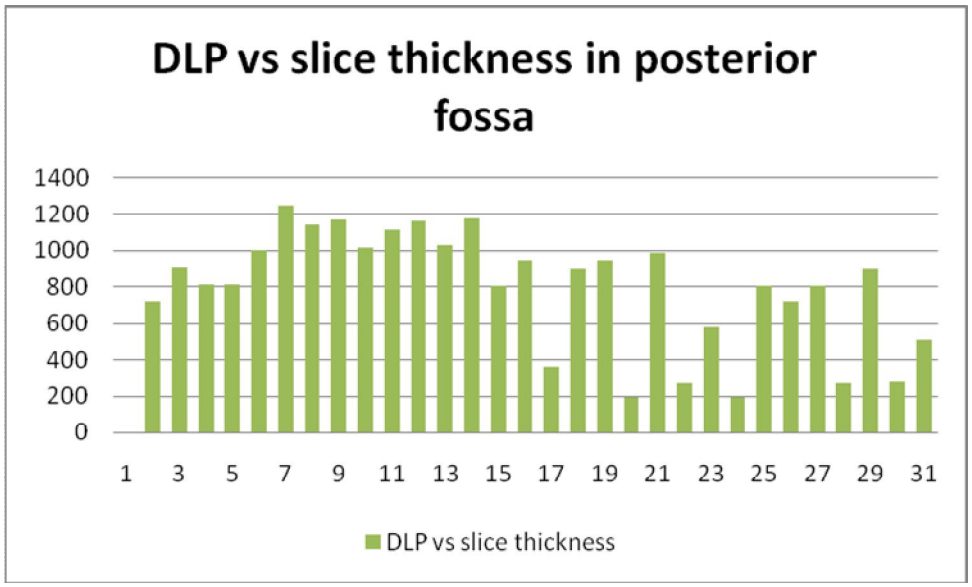


**Figure 4.6 DLP vs  thickness  in posterior fossa**

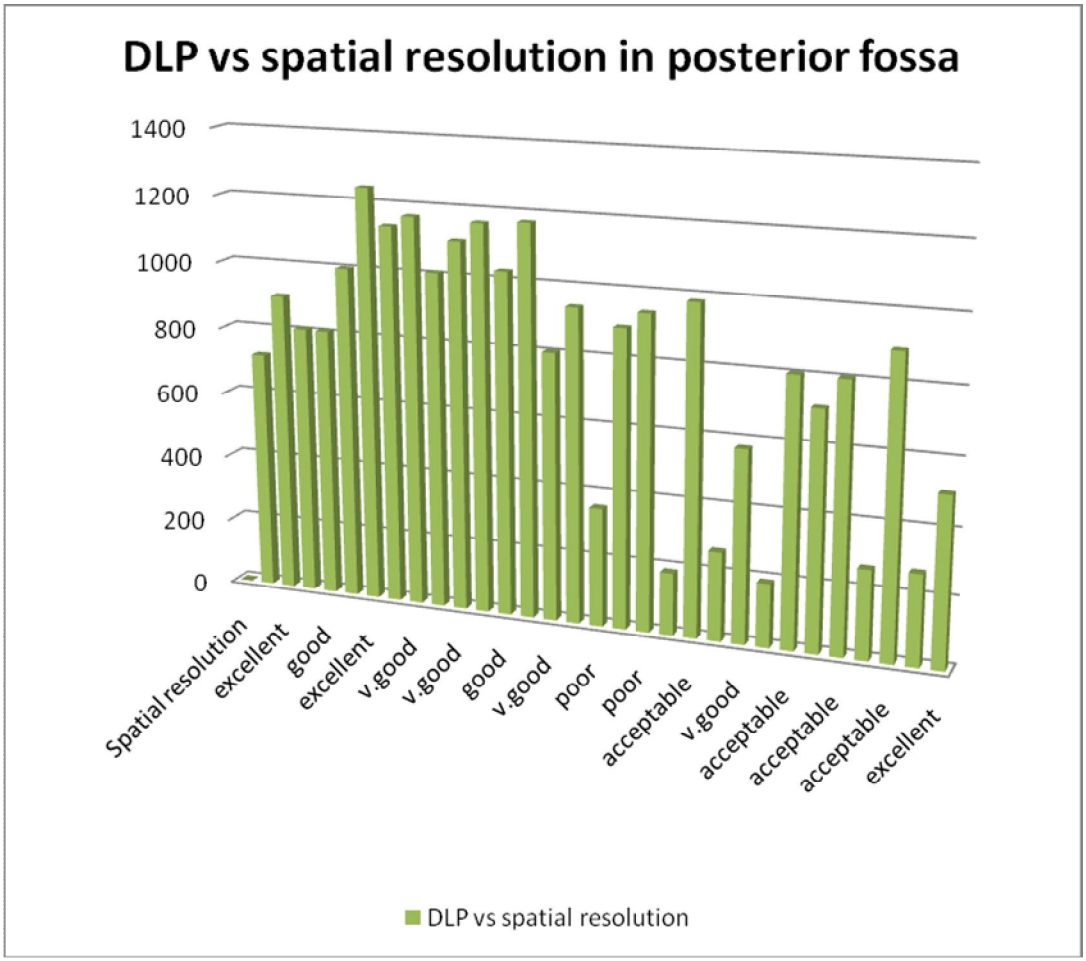


**Figure 4.7 DLP vs spatial resolution in posterior fossa**

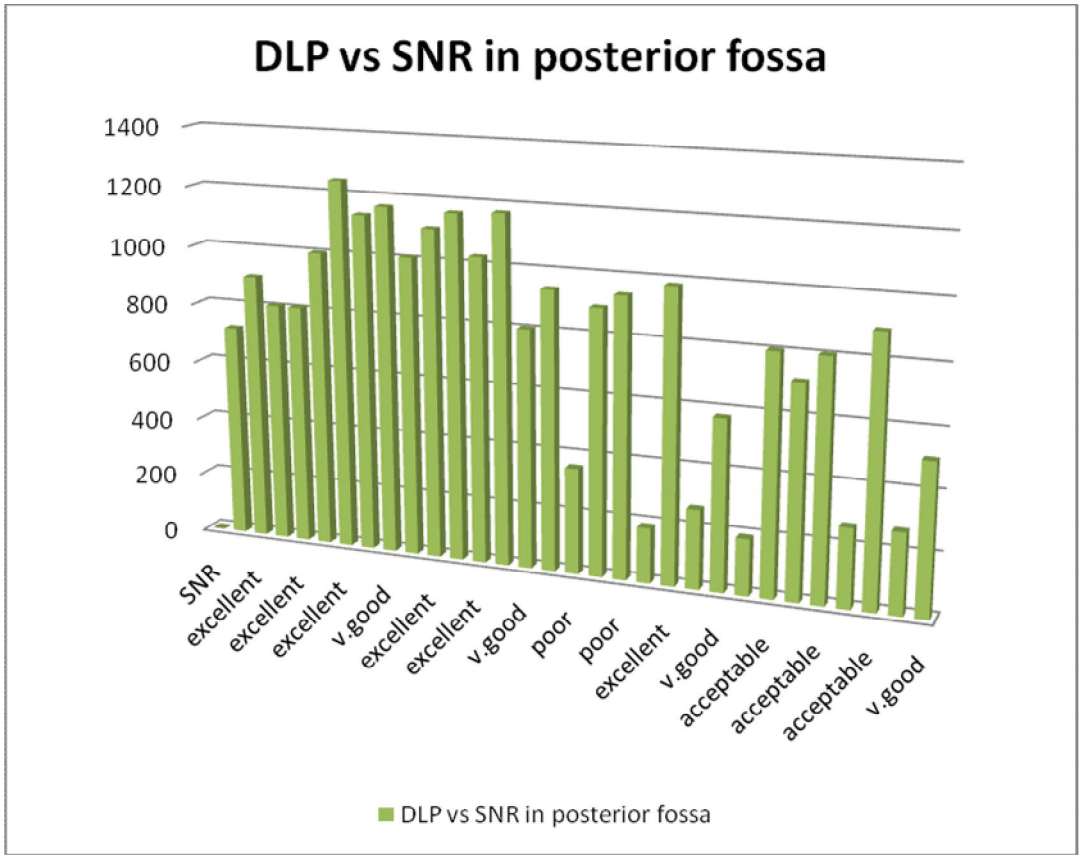


**Figure 4.8 DLP vs  SNR in posterior fossa**

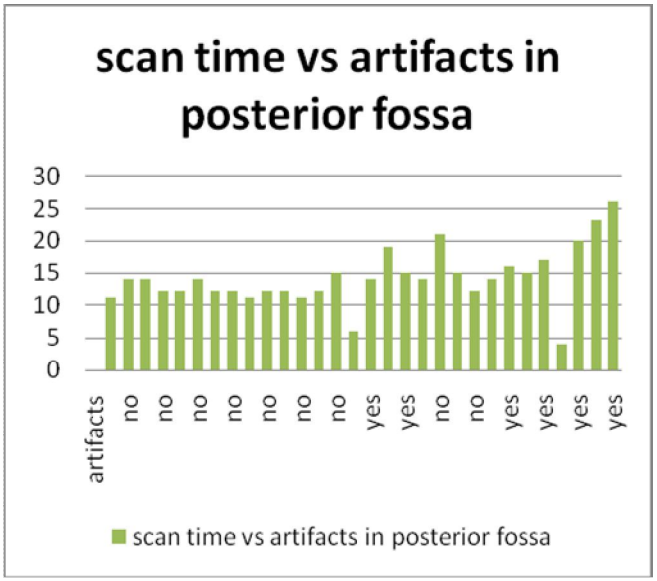


**Figure 4.9 Scan time vs artifacts in posterior fossa**

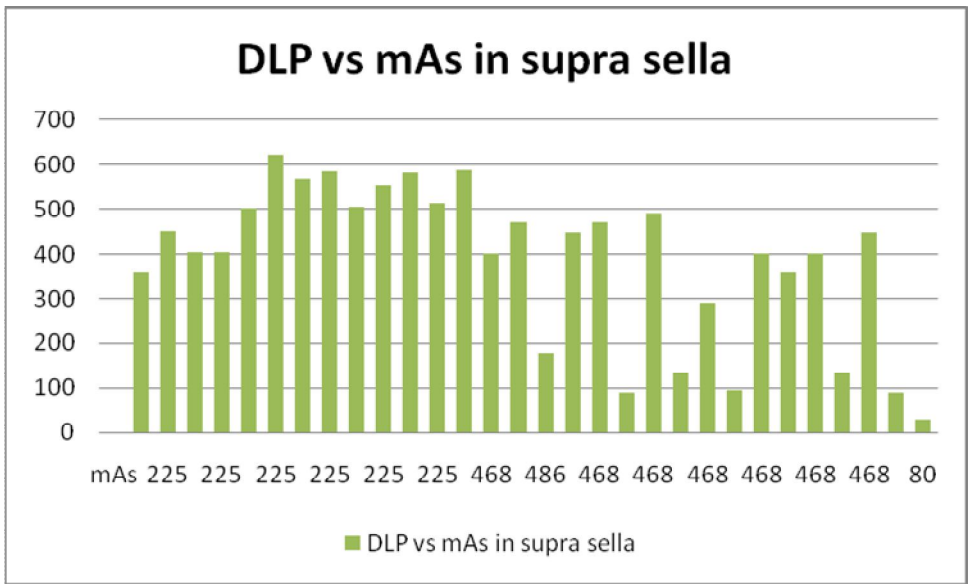


**Figure 4.10 Dlp vs mAs in supra sella**

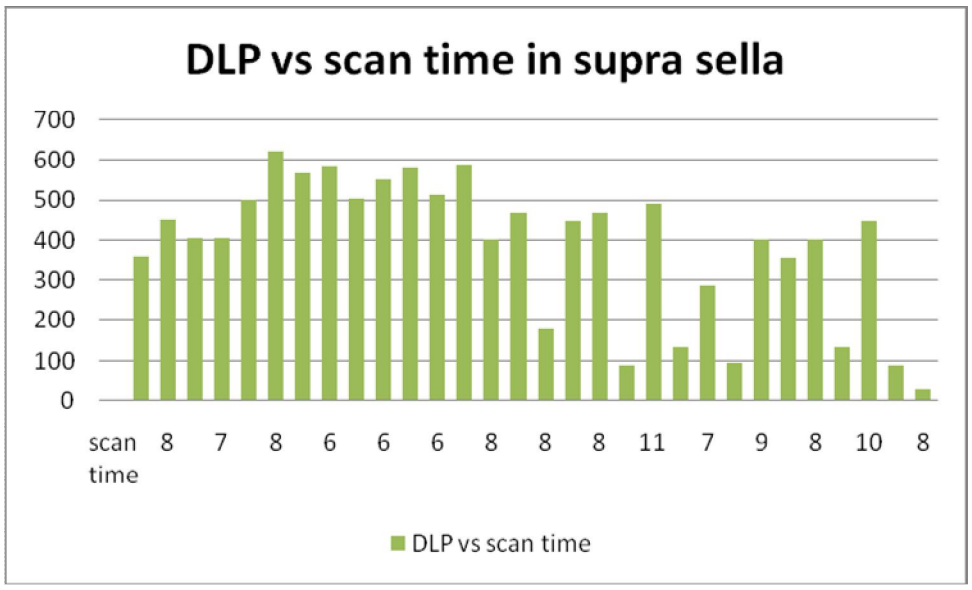


**Figure 4.11 Dlp vs Scan time in supra sella**

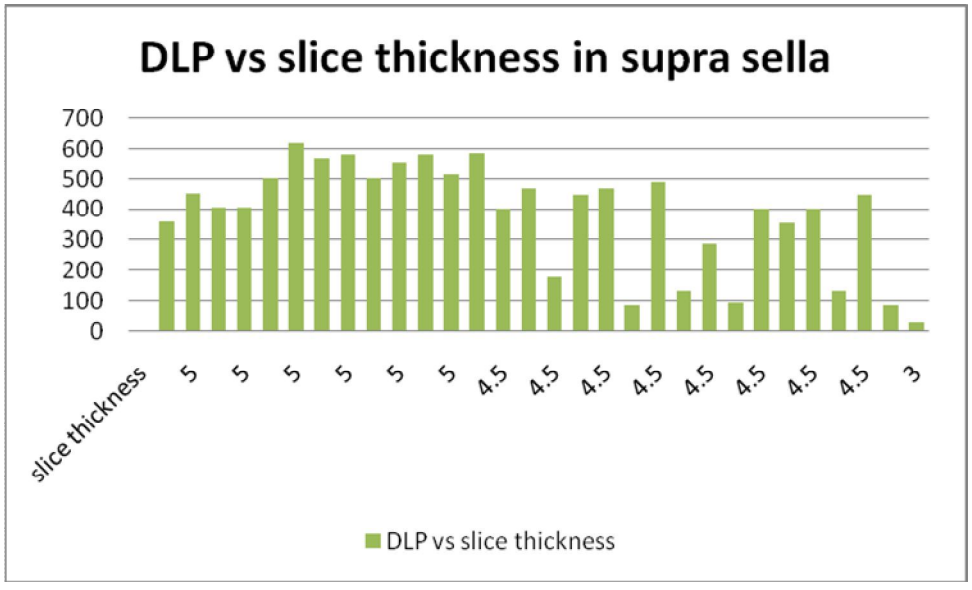


**Figure 4.12 Dlp vs slice thickness in supra sella**

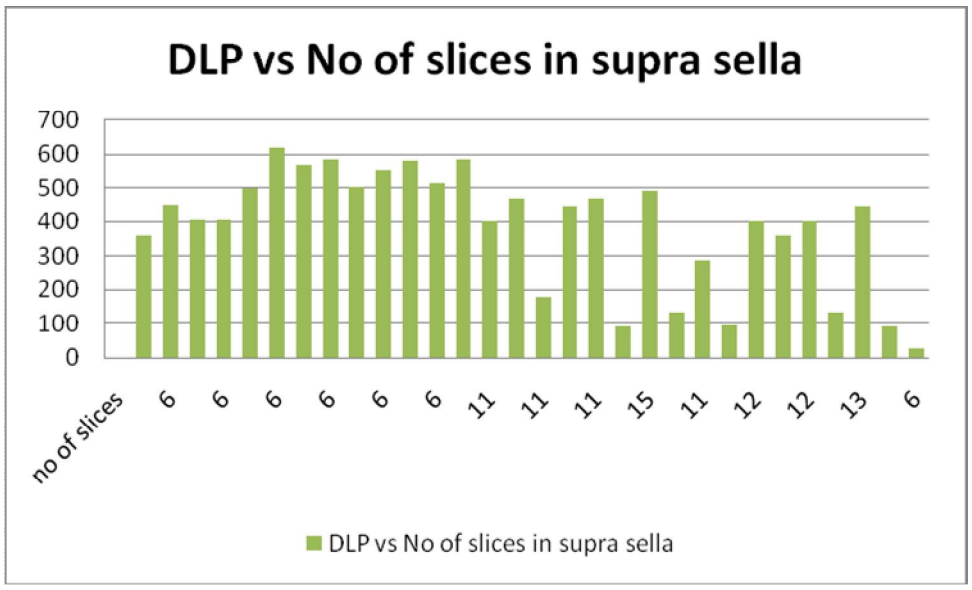


**Figure 4.13 Dlp vs  No of slices in supra sella**

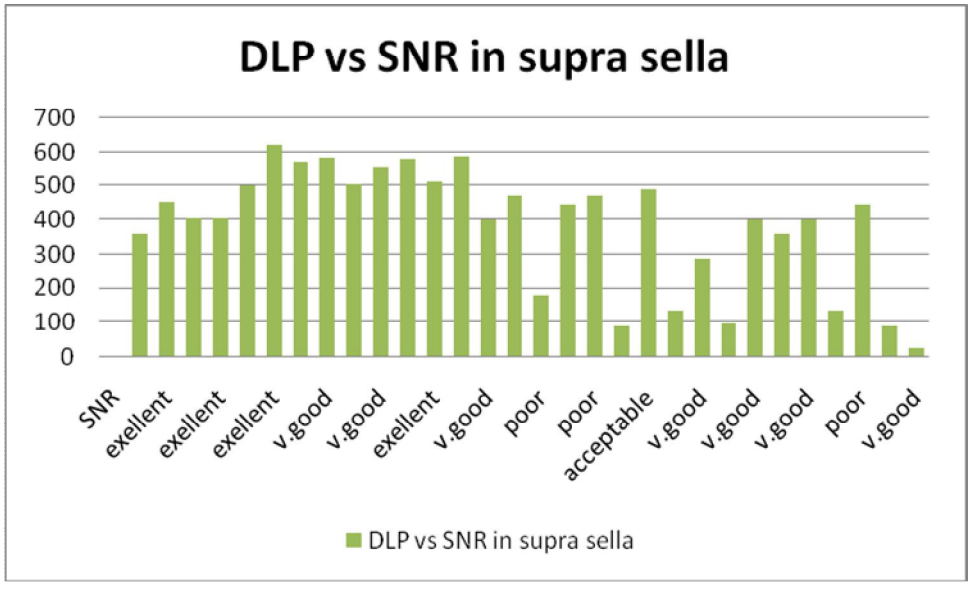


**Figure 4.14 Dlp vs SNR in supra sella**

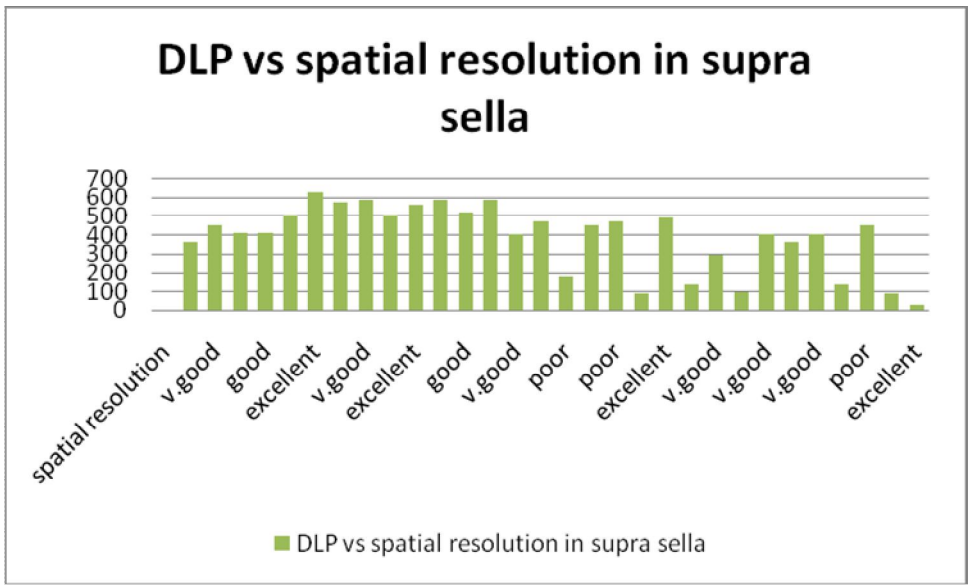


**Figure 4.15 Dlp vs spatial resolution  in supra sella**

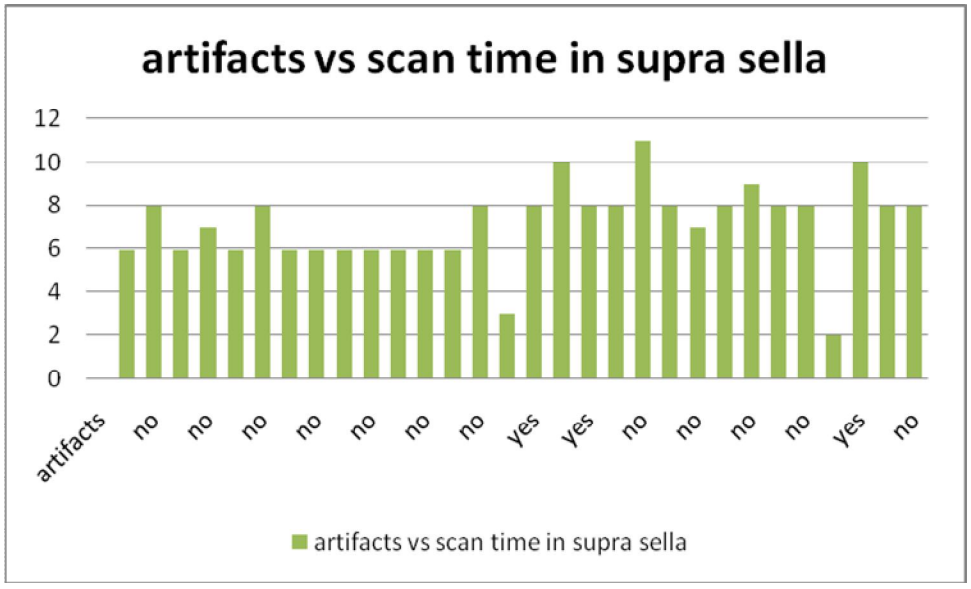


**Figure 4.16 artifacts vs scan time in supra sella**

# Chapter Five

## 5.1 Discussion:

In this thesis information taken from patients who underwent CT brain study, the data taken for 30 patients for posterior fossa and supra sella region each for(kv, mAs, CTDI, DLP, scan time, slice thickness and number of slices) we focus on radiation dose (DLP) and how it influences by mAs , scan time , slice thickness and number of slices. Also we compare between DLP and image quality(SNR and spatial resolution), SNR and spatial resolution evaluated subjectively by four radiologist whom they relatively visualize the picture and classified in to five grades(excellent, v.good, good, acceptable and poor) . Also a comparison made between artifacts and scan time.

## 5.2Conclusion:

The study showed that there is a variation between different CT scan units used in radiation dose and image quality. Also it showed that the radiation dose generally increase with mAs, scan time, slice thickness and the number of slices and showed that the image quality increases with radiation dose, However there is an existence of 20% of photographs having acceptable, good and very good in quality when we reduce the radiation dose to the half . Also The study showed that artifacts generally increases as the exposure time increases and has a close association with movement of the patient.

## 5.3Recommendations:

There should be highly qualified staff for processing CT scan radiography.

Using of different protocols for scanning  for adult and pediatric.

Reducing the radiation dose while keeping high image quality.

Reducing the scan time as possible as it could.

Regular quality control for CT equipments.

## References :

*Ambrose J. Computerized transverse axial scanning (tomography): Part 2. Clinical application. Br J Radiol 1973;46:1023–47.*

*Brooks RA, Di Chiro G. Principles of computer assisted tomography (CAT) in raxcvbhjioph2diographic and radioisotropic imaging. Phys Med Biol 1976;21:689–732*

Brenner DJ, Doll R, Goodhead DT, et al. Cancer risks attributable to low doses of ionizing radiation: assessing what we really know. Proc Natl Acad Sci U S A 2003;100:13761-6.

Brenner DJ, Elliston CD, Hall EJ, Berdon WE. Estimates of the cancer risks from pediatric CT radiation are not merely theoretical. Med Phys 2001;28:2387-8.

Cardis E, Vrijheid M, Blettner M, et al. The 15-country collaborative study of cancer risk among radiation workers in the nuclear industry: estimates of radiationrelated cancer risks. Radiat Res 2007;167: 396-416.

“Computed tomography – Definition from the Merriam-Webster Online Dictionary”. Retrieved 2009-08-18.

Computed medical imaging. Nobel lectures in physiology or medicine 1971–1980; 568–86.

CT IMAGE QUALITY BY Wil Reddinger, M.Sc. R.T.(R)(CT) copy right April 1998.

Groves AM, Owen KE, Courtney HM, et al. 16-Detector multislice CT: dosimetry estimation by TLD measurement compared with Monte Carlo simulation. Br J Radiol 2004;77:662-5.

Giles J. Study warns of ‘avoidable’ risks of CT scans. Nature 2004;431:391.

Health risks from exposure to low levels of ionizing radiation — BEIR VII. National Academies Press, 2005Washington, DC:.\

Herman, G. T., Fundamentals of computerized tomography: Image reconstruction from projection, 2 nd edition, Springer, 2009.

**http://www.sprawls.org/resources/CTIQDM/**

*Hounsfield GN. Computerized transverse axial scanning (tomography): Part 1. Description of system. Br J Radiol 1973;46:1016–22.*

Idem. Risk of cancer after low doses of ionising radiation: retrospective cohort study in 15 countries. BMJ 2005;331:77.

Martin CJ, Sutton DG, Sharp PF. Balancing patient dose and image quality. **Appl Radiat Isot 1999;50:1-19.**

McNitt-Gray MF. AAPM/RSNA physics tutorial for residents — topics in CT: radiation dose in CT. Radiographics 2002; 22:1541-53.

Mettler FA Jr, Wiest PW, Locken JA, Kelsey CA. CT scanning: patterns of use and dose. J Radiol Prot 2000;20:353-9

Mitelman F, Johansson B, Mertens FE. Mitelman database of chromosome aberrations in cancer. Cancer Genome Anatomy Project, 2007. (Accessed November 5, 2007, at http://cgap.nci.nih.gov/ Chromosomes/Mitelman.)

n engl j med 357;22 www.nejm.org 2278 november 29, 2007.

Paterson A, Frush DP, Donnelly LF. Helical CT of the body: are settings adjusted for pediatric patients? AJR Am J Roentgenol 2001;176:297-301.

Pierce DA, Preston DL. Radiationrelated cancer risks at low doses among atomic bomb survivors. Radiat Res 2000; 154:178-86.

Preston DL, Ron E, Tokuoka S, et al. Solid cancer incidence in atomic bomb survivors: 1958-1998. Radiat Res 2007;168: 1-64.

Preston DL, Shimizu Y, Pierce DA, Suyama A, Mabuchi K. Studies of mortality of atomic bomb survivors. Report 13: Solid cancer and noncancer disease mortality: 1950-1997. Radiat Res 2003;160:381- 407.

Preston DL, Pierce DA, Shimizu Y, et al. Effect of recent changes in atomic bomb survivor dosimetry on cancer mortality risk estimates. Radiat Res 2004;162:377- 89.

Polo SE, Jackson SP (March 2011). "Dynamics of DNA damage response proteins at DNA breaks: a focus on protein modifications". Genes Dev.

The Measurement, reporting, and management of radiation Dose in CT "in a single dose parameter that reflects the risk of a nonuniform exposure in terms of an equivalent whole-body exposure."Report of AAPM task group 23 of the diagnostic imaging council CT committee (January 2008)

The British Journal of Radiology, 79 (2006), 5–8 *E* 2006 The British Institute of Radiology
DOI: 10.1259/bjr/29444122

*www.RadiologyInfo.org/en/info.cfm?pg=angioct).*

www.mayfieldclinic.com.

## Appendix (1)

## Questionnaire

Name…….sex…….age…….. date……..

Protocol used……

**Readings in posterior fossa region:**

| Kv | MAs | CTDI | DLP | Scan time | Slice thickness | No of slice |
|---|---|---|---|---|---|---|
| | | | | | | |

## Readings in supra sella region:

| Kv | MAs | CTDI | DLP | Scan time | Slice thickness | No of slice |
|---|---|---|---|---|---|---|
| | | | | | | |

## Image quality:

## In posterior fossa region:

(a) SNR

Excellent ( ) v.good ( ) good ( ) acceptable ( ) poor( )

(b)Artifacts: yes ( ) No ( )

(c)Spatial resolution:

Excellent ( ) v.good ( ) good ( ) acceptable ( ) poor( )

## In supra sella region:

(a) SNR

Excellent ( ) v.good ( ) good ( ) acceptable ( ) poor( )

(b)Artifacts: yes ( ) No ( )

(c)Spatial resolution:

Excellent ( ) v.good ( ) good ( ) acceptable ( ) poor( )

## Equipment information:

Manufacturer…… manufacture date……

Type of machine……year of installation…….

Maximum kv……..maximum mAs……..

# Appendix (2)

# Reading in POSTERIOR fossa

| mAs | DLP | scan time | slice thickness | No of slices | SNR | Spatial resolution | artifacts |
|---|---|---|---|---|---|---|---|
| 225 | 719.6 | 11 | 5 | 11 | good | good | no |
| 225 | 903.6 | 14 | 5 | 11 | excellent | excellent | no |
| 225 | 810.2 | 14 | 5 | 11 | excellent | excellent | no |
| 225 | 809.4 | 12 | 5 | 11 | excellent | good | no |
| 225 | 1002 | 12 | 5 | 11 | acceptable | v.good | no |
| 225 | 1244.9 | 14 | 5 | 11 | excellent | excellent | no |
| 225 | 1137.3 | 12 | 5 | 11 | good | good | no |
| 225 | 1169.3 | 12 | 5 | 11 | v.good | v.good | no |
| 225 | 1010 | 11 | 5 | 11 | excellent | v.good | no |
| 225 | 1108.7 | 12 | 5 | 11 | excellent | v.good | no |
| 225 | 1164 | 12 | 5 | 11 | excellent | acceptable | yes |
| 225 | 1029.3 | 11 | 5 | 11 | excellent | good | no |
| 225 | 1174.7 | 12 | 5 | 11 | excellent | v.good | no |
| 468 | 804.78 | 15 | 4.5 | 21 | v.good | v.good | no |
| 487 | 941.25 | 6 | 4.5 | 33 | acceptable | acceptable | yes |
| 468 | 357.68 | 14 | 4.5 | 21 | poor | poor | yes |
| 468 | 894.2 | 19 | 4.5 | 26 | poor | poor | yes |
| 468 | 941.2 | 15 | 4.5 | 21 | poor | poor | yes |
| 468 | 187.84 | 14 | 4.5 | 21 | excellent | excellent | no |
| 468 | 983.56 | 21 | 4.5 | 29 | excellent | acceptable | no |
| 468 | 268.26 | 15 | 4.5 | 21 | good | acceptable | yes |
| 468 | 577.7 | 12 | 4.5 | 21 | v.good | v.good | no |
| 468 | 191 | 14 | 4.5 | 21 | acceptable | acceptable | yes |
| 468 | 804.79 | 16 | 4.5 | 24 | acceptable | acceptable | yes |
| 468 | 715.36 | 15 | 4.5 | 21 | acceptable | acceptable | yes |
| 468 | 804.78 | 17 | 4.5 | 24 | acceptable | acceptable | yes |
| 468 | 268.26 | 4 | 4.5 | 10 | poor | poor | yes |
| 468 | 894.2 | 20 | 4.5 | 25 | acceptable | acceptable | yes |
| 80 | 273.34 | 23 | 7 | 13 | good | excellent | no |
| 130 | 507.64 | 26 | 7 | 16 | v.good | excellent | yes |

# Appendix (3)

## Readings in Supra sella

| mAs | CTDI | DLP | scan time | slice thickness | no of slices | | SNR | spatial resolution | artifacts |
|---|---|---|---|---|---|---|---|---|---|
| 225 | | 359.7 | 6 | 5 | | 6 | good | good | no |
| 225 | | 451.7 | 8 | 5 | | 6 | exellent | v.good | no |
| 225 | | 405.1 | 6 | 5 | | 6 | exellent | excellent | no |
| 225 | | 404.6 | 7 | 5 | | 6 | exellent | good | no |
| 225 | | 501 | 6 | 5 | | 6 | acceptable | v.good | no |
| 225 | | 622.43 | 8 | 5 | | 6 | exellent | excellent | no |
| 225 | | 568.7 | 6 | 5 | | 6 | good | good | no |
| 225 | | 584.7 | 6 | 5 | | 6 | v.good | v.good | no |
| 225 | | 505 | 6 | 5 | | 6 | exellent | v.good | no |
| 225 | | 554.3 | 6 | 5 | | 6 | v.good | excellent | no |
| 225 | | 582 | 6 | 5 | | 6 | good | good | no |
| 225 | | 514.7 | 6 | 5 | | 6 | exellent | good | no |
| 225 | | 587.3 | 6 | 5 | | 6 | exellent | v.good | no |
| 468 | | 402.39 | 8 | 4.5 | | 11 | v.good | v.good | no |
| 486 | | 470.15 | 3 | 4.5 | | 17 | v.good | v.good | no |
| 486 | | 178.84 | 8 | 4.5 | | 11 | poor | poor | yes |
| 468 | | 447.1 | 10 | 4.5 | | 14 | v.good | v.good | no |
| 468 | | 470.6 | 8 | 4.5 | | 11 | poor | poor | yes |
| 468 | | 89.42 | 8 | 4.5 | | 11 | exellent | excellent | no |
| 468 | | 491.78 | 11 | 4.5 | | 15 | acceptable | excellent | no |
| 468 | | 134.13 | 8 | 4.5 | | 11 | v.good | v.good | no |
| 468 | | 288.9 | 7 | 4.5 | | 11 | v.good | v.good | no |
| 468 | | 95.48 | 8 | 4.5 | | 11 | v.good | v.good | no |
| 468 | | 402.39 | 9 | 4.5 | | 12 | v.good | v.good | no |
| 468 | | 357.68 | 8 | 4.5 | | 11 | v.good | v.good | no |
| 468 | | 402.39 | 8 | 4.5 | | 12 | v.good | v.good | no |
| 468 | | 134.3 | 2 | 4.5 | | 2 | poor | poor | yes |
| 468 | | 447.1 | 10 | 4.5 | | 13 | poor | poor | yes |
| 130 | | 89.66 | 8 | 3 | | 6 | v.good | good | no |
| 80 | | 27.89 | 8 | 3 | | 6 | v.good | excellent | no |